TARGETED DELETION OF PTP4A3 INHIBITS COLON CARCINOGENESIS AND ANGIOGENESIS

by

Mark W. Zimmerman

B.S., Rochester Institute of Technology, 2006

M.B.A., Rochester Institute of Technology, 2007

Submitted to the Graduate Faculty of the

University of Pittsburgh School of Medicine

in partial fulfillment

of the requirements for the degree of

Doctor of Philosophy

University of Pittsburgh

2013

UNIVERSITY OF PITTSBURGH

SCHOOL OF MEDICINE

This dissertation was presented

by

Mark W. Zimmerman

It was defended on

April 15, 2013

and approved by

Don B. DeFranco, Ph.D.
Committee Chair
Professor, Department of Pharmacology and Chemical Biology

Thomas E. Smithgall, Ph.D.
Professor and Chair, Department of Microbiology and Molecular Genetics

Nathan Bahary, M.D., Ph.D.
Assistant Professor, Department of Medicine, Division of Hematology/Oncology

Jeffery S. Isenberg, M.D.
Associate Professor, Vascular Medicine Institute, Division of Pulmonary, Allergy and Critical Care Medicine

John S. Lazo, Ph.D.
Professor, Department of Pharmacology, University of Virginia

Gregg E. Homanics, Ph.D.
Professor, Department of Anesthesiology

TARGETED DELETION OF PTP4A3
INHIBITS COLON CARCINOGENESISAND ANGIOGENESIS

Mark W. Zimmerman, Ph.D.

University of Pittsburgh, 2013

Protein tyrosine phosphatase 4a3 (*Ptp4a3*) is an enigmatic member of the *Ptp4a* family of prenylated protein tyrosine phosphatases, which are highly expressed in many human cancers. Despite strong correlations with tumor metastasis and poor patient prognosis, there is very limited understanding of this gene family's role in malignancy. A gene targeted mouse knockout model for *Ptp4a3*, the most widely studied *Ptp4a* family member, was created. Mice deficient for PTP4A3 were grossly normal. However, fewer homozygous-null males were observed at weaning and they maintained a decreased body mass into adulthood.

Although PTP4A3 is normally associated with late-stage cancer and metastasis, increased *Ptp4a3* mRNA was observed in the colon of C57BL/6J mice immediately following treatment with the carcinogen azoxymethane. A well characterized murine colitis-associated colon cancer model was used to investigate the role of PTP4A3 in malignancy. Wildtype mice treated with azoxymethane and dextran sodium sulfate (AOM/DSS) developed approximately 7-10 tumors per mouse in the distal colon. The resulting tumor tissue had 4-fold more *Ptp4a3* mRNA relative to normal colon epithelium and increased PTP4A3 protein. *Ptp4a3*-null mice developed 50% fewer colon tumors than wildtype mice after exposure to AOM/DSS. Tumors from the *Ptp4a3*-null mice had elevated levels of both IGF1Rβ and c-MYC compared to tumors replete with PTP4A3, suggesting an enhanced cell signaling pathway engagement in the absence of the phosphatase. Furthermore, c-MYC activity was able to increase *Ptp4a3* gene expression in a

fibroblast cell culture model. These results provide the first definitive evidence implicating PTP4A3 in colon carcinogenesis and highlight the potential value of the phosphatase as a therapeutic target for early stage malignant disease.

Interestingly, PTP4A3 is also expressed in the tumor vasculature and has been proposed to be a direct target of vascular endothelial growth factor (VEGF) signaling in endothelial cells. Compared to wildtype controls, colon tumor tissue isolated from *Ptp4a3*-null mice revealed reduced microvessel density demonstrated by CD31 staining. Vascular cells derived from *Ptp4a3*-null tissue explants exhibited decreased invasiveness *ex vivo* compared to wildtype tissues. When primary endothelial cells were isolated and cultured *in vitro*, *Ptp4a3*-null cells displayed less migration compared to wildtype cells and loss of VEGF-induced phosphorylation of SRC protein. Reduced migration and SRC activation were also observed when human endothelial cells were treated with a small molecule inhibitor of PTP4A3. These findings strongly support a role for PTP4A3 as an important contributor to cancer progression as well as endothelial cell function *in vivo*.

TABLE OF CONTENTS

LIST OF TABLES

LIST OF FIGURES

PREFACE

The time I have spent at the University of Pittsburgh has been the most challenging and rewarding experience of my life. I have truly enjoyed my time in the Molecular Pharmacology training program and cannot speak highly enough about its mission, leadership, and dedicated faculty and staff. The work presented here would not have been possible without the support of many advisors, colleagues, friends and family.

I would first like to thank my thesis advisors John Lazo and Gregg Homanics for the amazing opportunity they have given me. The confidence and scientific abilities that I possess are a direct reflection of their mentorship and constant encouragement. I would also like to thank all past and present members of the Lazo and Homanics laboratories. The outstanding co-workers I have had the pleasure of working with have all contributed to my success in some way and I could not be more grateful. The willingness of everyone I have worked with to unconditionally give me their time and effort whenever it was needed is both humbling and inspiring beyond belief.

I would like to thank my thesis committee members Don Defranco, Tom Smithgall, Nathan Bahary and Jeff Isenberg for constantly providing their valuable time and input to make my project a success. Their insightful comments, suggestions, and critiques have been an incredible resource and have greatly contributed to my development as a scientist. I have also met several collaborators that I have learned a great deal from, and they greatly contributed to

the significance of this research. I would especially like to thank Carolyn Ferguson, Bruce Pitt, Karla Wasserloos, Julie Chandler, Eric Lagasse and Ed Prochownik as their involvement in this project has been particularly important and much appreciated.

Special thanks are also necessary for the faculty and staff that of the graduate program. The leadership group of Bruce Freeman, Patrick Pagano and Guillermo Romero has provided a positive and rigorous training environment that I have greatly enjoyed being a part of. I also extend sincere thanks to Pat Smith, Cindy Duffy, Michelle Darabant, Bev Savage and Jen Walker. Their constant efforts and assistance went above and beyond and is deeply appreciated.

Finally, I would like to thank my family which has grown considerably since I moved to Pittsburgh. To my parents, in-laws, brothers and sisters...I could not have done this without your love and support. To my wife and best friend, Jamie, thank you for your love, support, encouragement and being by my side this entire time. It has meant the world to me.

Tempus fugit.

1.0 INTRODUCTION

1.1 PROTEIN TYROSINE PHOSPHATASES

Protein phosphorylation is one of the key mechanisms by which cells transmit signals in response to extracellular stimuli [1]. Phosphorylation of specific amino acid residues directly regulates protein conformation and dynamics that ultimately control cellular phenotype. The covalent addition of phosphate groups typically occurs on the hydroxyamino acids tyrosine, serine, and threonine. These reversible phosphorylation events are controlled by an intricate network of protein kinases and phosphatases, which add and remove phosphate, respectively. This constant balance between kinase and phosphatase activity is essential for cells to not only respond to their environment but also to maintain normal functioning and homeostasis.

In humans, the protein tyrosine phosphatase (PTP) superfamily is a group of 107 genes either demonstrated or predicted to have phosphatase activity [2]. Homologs of most of these genes are found in mice and other mammals indicating the importance and complexity of maintaining balance in phosphorylation signaling. This family is divided into four classes based on their structure and catalytically active amino acid residue. The classic targets for PTP enzymatic activity are tyrosine residues on various proteins. However, some family members are classified as dual-specificity phosphatases (DSP) due to their ability to act on the shorter side chains of serine and threonine residues. Other members of the PTP family have the ability to

dephosphorylate non-protein substrates such as phosphoinositide. Collectively, the PTPs are an interesting and complex group of enzymes that have an integral role in the biology of virtually every living organism.

1.2 PHOSPHATASES AND CANCER

While dynamic phosphorylation facilitates the processes essential for normal cellular functions, abnormal phosphorylation has been observed in most pathological conditions including hypertension, diabetes, neurodegeneration, and cancer among others [3]. The role of phosphatases in cancer is particularly interesting because aberrant phosphorylation is fundamentally causal in many malignancies. At least 40 human PTPs have been described as deleted or overexpressed in various cancers to date, with potential roles in cellular proliferation, migration, invasion, and survival [4]. Several phosphatases have known roles in tumor suppression, and disruption of the activity of these genes can have a causal role in cancer progression [5]. On the other hand, approximately 22 PTPs are thought to have oncogenic properties and may contribute to carcinogenesis and metastasis. This group includes: PTP1B [6], CDC25 [7], and PTP4A3 [8]; all of which are currently under investigation as therapeutic targets. A more comprehensive understanding of the enzymology and role of these genes in cancer should shed considerable light on opportunities to effectively treat the disease.

Therapeutically targeting phosphorylation events can be an effective approach to treat or prevent cancer. Somewhat pragmatically, small molecule inhibitors of kinases were initially developed for cancer treatment – 17 small molecule kinase inhibitors are now approved by the FDA and many more under clinical investigation [9]. Deregulation of kinase activity is among

the first well characterized etiologies of malignancy and the relatively high diversity among the 516 putative kinases affords considerable opportunity for therapeutic intervention. Potent and specific molecules for the inhibition of phosphatases are substantially more challenging to develop; a result partially attributable to high conservation of the catalytic domain among various PTPs. Despite this obstacle, there remains a great deal of therapeutic potential within the PTP family of genes due to their critical roles in disease.

1.3 PTP4A FAMILY PHOSPHATASES

1.3.1 Discovery of *Ptp4a1*

The *Ptp4a* family of protein tyrosine phosphatases was originally identified when *Ptp4a1* was observed as an immediate early gene expressed in regenerating liver cells following partial hepatectomy in rodents [10]. As a result of this discovery, it is given the acronym Phosphatase of Regenerating Liver (or PRL), which is commonly used in the literature. The nature of this expression suggests a potential mitogenic activity, especially considering *Ptp4a1* is also expressed in insulin treated rat hepatoma cells as well as a number of human cancer cell lines [11]. While associated with proliferation in the liver, *Ptp4a1* is expressed in differentiated intestinal cells, indicating a complex regulatory system that has yet to be fully understood. The mouse *Ptp4a2* and *Ptp4a3* genes were subsequently identified as closely related family members [12]. Together, these genes make up a subfamily of the Class I (VH1-like) DSPs, with all three members conserved throughout all mammalian species.

1.3.2 *Ptp4a* gene structure and homology

The PTP4A gene products are very similar in structural and domain characteristics (Fig. 1). They are all around 21 kDa in mass and share the characteristic phosphatase WPD-loop and P-loop, which make up the PTP domain. The WDP-loop is a conserved sequence involved in substrate recognition and binding, while the P-loop is the site that catalyzes hydrolysis of the inorganic phosphate. They also share a polybasic region and a C-terminal prenylation motif (CAAX box), which makes them the only phosphatases known to be prenylated [12]. The polybasic region provides a cluster of positive charges that is thought to participate in lipidation [13]. The exact mechanism and importance of this prenylation is not well characterized but it is important for intracellular localization of the PTP4A protein products [14].

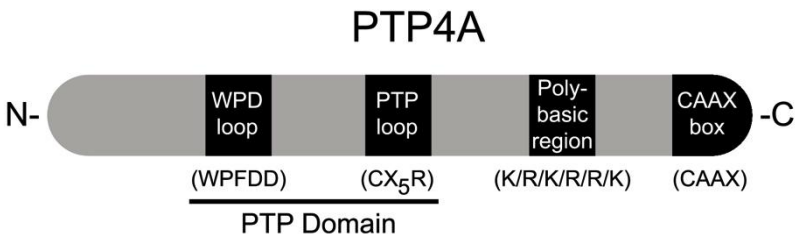

Figure 1. PTP4A protein domains

The PTP4A family proteins share several domains that are likely important for their enzymatic function. The WPD and PTP loops are known to facilitate the removal of phosphate groups from various substrates. The poly-basic region and the C-terminal CAAX box are likely important for cellular localization the proteins. PTP4A is the only phosphatase family known to be prenylated.

The localization of PTP4A proteins in most cell types is usually observed at the plasma membrane and in endosomal structures [14]. This is consistent with prenylation as the addition of lipid modifications typically targets proteins to membranous structures. Nuclear localization of PTP4A3 has also been reported [15], which could reflect association with the nuclear

membrane. PTP4A3 protein cycles back and forth between the nucleus and plasma membrane in human myeloma cells in a cell cycle-dependent manner [15]. In these cells, nuclear localization is primarily seen during G_0/G_1 phase, while localization to cytoplasmic regions is seen during S and G_2/M phases. This localization pattern may be particularly relevant since increases in PTP4A3 expression are associated with G_1 cell cycle arrest in several cell types [16]. The ability to localize to both the plasma membrane and the nucleus supports previously reported findings that PTP4A3 can have a diverse range of effects including cell migration as well as roles in gene transcription and cell cycle progression.

Farnesyl transferase is thought to control PTP4A C-terminal prenylation and inhibitors of farnesyl transferase prevent membrane localization of both PTP4A1 and PTP4A3 [17]. Farnesylation has also been reported for PTP4A2, which can then interact with but is not likely a substrate for, the beta-subunit of Rab geranylgeranyltransferase II [18]. Classical CAAX (where A is an aliphatic residue and X is any amino acid) prenylation involves lipidation at the cysteine residue followed by cleavage of the AAX tripeptide. With PTP4A3 (CCVM), however, an alternative mechanism may be operative in which farnesylation of the first cysteine is followed by palmitoylation of the proximal cysteine with no subsequent proteolysis [19]. This alternative mechanism expands the potential diversity of PTP4A3 signaling and may be an additional form of protein regulation through the reversible addition of palmitate.

While there exists a high degree of primary amino acid homology among PTP4A family members (Fig. 2), there is relatively little homology to the other PTP families. Structurally, PTP4A is most similar to the phosphatases VHR and PTEN [20]. High sequence and structural conservation among the three family members, particularly around the catalytic domain, suggests similar substrates and enzymology.

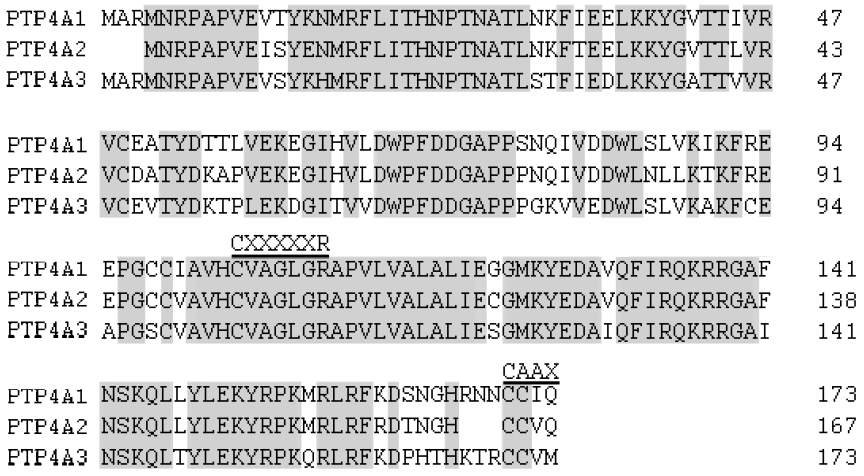

Figure 2. Amino acid sequence alignment of PTP4A family proteins

Amino acid sequence alignment of all three PTP4A family proteins with conserved residues shaded in gray. All three protein sequences are than 70% identical in amino acid composition with considerable homology surrounding the catalytic domain.

There is, however, a high degree of evolutionary conservation among mammalian species, which could imply the preservation of non-redundant biological roles. For example, the human and mouse isoforms of PTP4A1 and PTP4A2 are completely identical. The homologs of human and mouse PTP4A3 are 96% identical differing at only 6 amino acid residues (Fig. 3). Possibly these phosphatases have unique developmental or tissue specific roles.

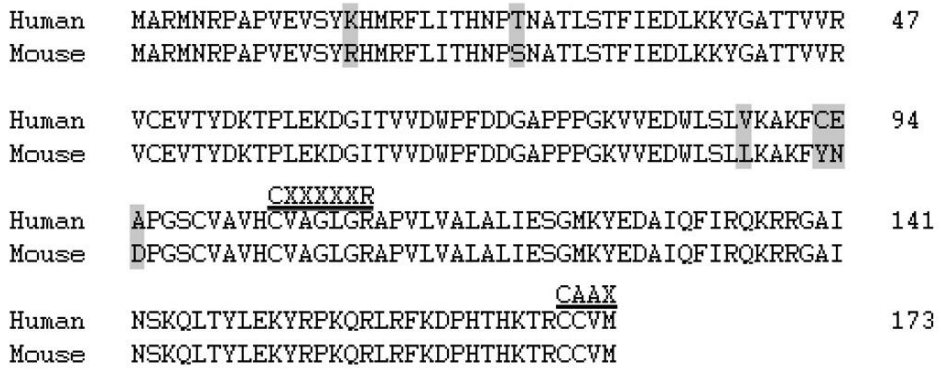

Figure 3. Amino acid sequence alignment of human and mouse PTP4A3 homologs

Amino acid sequence alignment of human and mouse PTP4A3 proteins with differing residues shaded in gray. Only 6 residue discrepancies in the N-terminal side of the proteins are apparent making the final products 96% identical.

1.3.3 Endogenous and developmental expression of *Ptp4a* genes

The antibodies currently available to detect endogenous PTP4A protein expression produce poor signal strength and recognize a number of other proteins. Thus, most of the characterization of *Ptp4a* tissue expression has been performed by assaying transcript levels via Northern blot or *in situ* hybridization. *Ptp4a1* and *Ptp4a2* are each thought to have ubiquitous transcript expression in most adult and embryonic tissue types. In adults, *Ptp4a1* is expressed at high levels in the stomach (pyloric region), small intestine, gallbladder, oviduct, testis, lung and adipose tissue [21]. Moderate levels of *Ptp4a1* are seen in most other tissues. High expression of *Ptp4a1* expression is observed in several embryonic tissues and is likely differentially regulated throughout development. In mouse embryos (E10.5-18.5), *Ptp4a1* mRNA is detectable in the brain, neural tube, and dorsal root ganglia and in several non-neuronal tissues, including the skeletal system [22]. The same report also describes *Ptp4a1* gene expression in various cell types

during cartilage differentiation. Another report that examined PTP4A1 protein levels demonstrated expression at variable time points in the developing intestine, specifically in villus enterocytes [23]. PTP4A1 protein is also detectable in the developing liver, esophagus, kidney and lung.

Prominent *Ptp4a2* expression levels are observed in most human tissues and cell types indicating it has the highest endogenous expression levels [21]. Mice deficient for functional *Ptp4a2* exhibit decreased body mass and abnormal placental development as a result of defective proliferation of the spongiotrophoblast and decidua layers [24]. The expression pattern of *Ptp4a2* during development has not been well characterized, although strong expression levels are observed in most fetal tissues.

Ptp4a3 was initially described as a heart and skeletal muscle specific phosphatase with lower levels of mRNA expression in the pancreas [25]. This restricted pattern of gene expression suggests a potential role in cardiovascular development. *Ptp4a3* expression has subsequently been reported in other normal and developing tissue types including high levels in the fetal heart, developing vasculature (endothelium), and pre-erythrocytes [26]. It is likely that expression of *Ptp4a3* is tightly regulated in a tissue and temporal specific manner that corresponds to changes in the cell state and exposure to environmental signals.

1.4 PTP4A3 EXPRESSION, REGULATION AND SIGNALING

1.4.1 *Ptp4a3* expression in human cancer

While all three *4a*-phosphatases are associated with various human cancers, *Ptp4a3* is the most strongly implicated family member in multiple human malignancies (Table 1). The first report of *Ptp4a3* in cancer emerged when high mRNA expression was reported in patient liver metastases derived from colorectal cancer [8]. Little or no expression is detectable in either the matched primary tumors or normal colon tissue. This finding suggests that *Ptp4a3* could serve as a biomarker or therapeutic target for the treatment of metastatic cancer. Subsequent reports indicate that *Ptp4a3* gene expression is elevated in primary colon tumors as well, and that high expression levels correlate with increased tumor invasiveness and patient morbidity [27, 28]. High expression of *Ptp4a3* is seen in cases of melanoma arising from the uvea [29], and expression in these tumors is a strong predictor of the occurrence of resulting liver metastases. Elevation of both *Ptp4a3* mRNA and protein are seen in glioma tissue, with higher levels corresponding to later stage disease [30].

Table 1. *Ptp4a* genes and associated cancer types

Ptp4a1		***Ptp4a2***		***Ptp4a3***	
Cancer Type	Reference	Cancer Type	Reference	Cancer Type	Reference
Liver	[31]	Lung	[32]	Colorectal	[8, 27, 28, 33]
Head & Neck	[34]	Breast	[35]	Head & Neck	[34, 36]
Pancreas	[37]	Hematopoietic	[38]	Gastric	[39-41]
		Pancreas	[37]	Liver	[42, 43]
		Prostate	[44]	Hematopoietic	[45, 46]
				Uvea	[29]
				Brain	[30]
				Breast	[47-50]
				Cervix	[51]
				Ovary	[52, 53]

Ptp4a3 expression is implicated in multiple malignancies of the digestive system. High expression of *Ptp4a3* is strongly associated with cancers of the head and neck, including tumors of the larynx and pharynx [54], as well as squamous cell esophageal cancer [34]. High *Ptp4a3* expression is also associated with poor survival in patients with nasopharyngeal carcinoma [36]. Multiple studies reveal that elevated *Ptp4a3* gene expression correlates with gastric tumor progression and is ultimately a predictor of metastasis [39-41]. *Ptp4a3* is also one of the most upregulated genes in gastrointestinal stromal tumors [55]. *Ptp4a3* is upregulated in hepatocellular carcinoma relative to normal tissue, and expression is closely related to microvessel density [43]. High *Ptp4a3* expression in hepatocellular carcinoma is also associated with low differentiation and poor patient prognosis[31, 42].

Ptp4a3 is also strongly associated with cancers of the hematopoietic system. *Ptp4a3* is highly expressed in nearly half of acute myelogenous leukemia (AML) cases, and is downregulated following treatment with a FLT3 inhibitor [45]. Ectopic overexpression restores the malignant phenotype suggesting a possible role in drug resistance. *Ptp4a3* is also among the most upregulated genes in chronic myelogenous leukemia (CML) with very little expression in

normal cells [46]. Although not well understood mechanistically, inhibition of BCR-ABL reduces *Ptp4a3* gene expression, but not in drug resistant cells indicating that *Ptp4a3* may be a downstream effector of BCR-ABL. Additionally, a subset of multiple myeloma patients expresses high *Ptp4a3*, all of which exhibit the presence of bone lesions [15, 56].

Multiple reports suggest *Ptp4a3* is highly expressed in a subset of breast cancers, with higher levels correlating with poor patient survival [47, 48, 50]. *Ptp4a3* expression is elevated in squamous cell carcinoma of the cervix, and is positively correlated to invasion of the surrounding lymph nodes [51]. High expression of *Ptp4a3* is also seen in ovarian cancer, with expression levels correlating to poor prognosis [52, 53].

1.4.2 Regulation of *Ptp4a3* gene expression in cancer

Ptp4a3 expression in cancer seems to be the result of a dynamic process rather than just a constitutive one, which would be consistent with an acute phase response gene first observed with family member *Ptp4a1* in liver. The factors enhancing or repressing *Ptp4a3* gene expression are likely to be tightly controlled by cell or tissue type, as well as the extracellular environment and a number independent stimuli. Interestingly, the first evidence for direct transcriptional regulation of *Ptp4a3* is through the tumor suppressor p53 [16]. Elevation of *Ptp4a3* gene expression in primary mouse embryonic fibroblasts (MEFs) is observed following exposure to genotoxic stress. Paradoxically, both ectopic *Ptp4a3* overexpression as well as short interfering RNA (siRNA) silencing of *Ptp4a3,* independent of p53 activity, is able to induce MEF cell cycle arrest [16]. This is strong evidence suggesting that PTP4A3 may be a key mediator of cell cycle progression particularly under conditions of cellular stress. In this regard,

PTP4A3 is reported to downregulate and reduce the activity of p53 in cancer cells through a negative feedback mechanism involving MDM2 and PIRH2 [57].

Another reported regulator of *Ptp4a3* gene expression is the pleiotropic cytokine Transforming Growth Factor β (TGFβ) [58]. The function of TGFβ in cancer and metastasis has been extensively detailed and could provide a meaningful rationale for the expression of *Ptp4a3* observed in various stages of cancer [59]. Binding of TGFβ to its receptors induces SMAD translocation to the nucleus where it binds and transcriptionally represses specific gene loci. TGFβ is proposed to regulate *Ptp4a3* expression through a SMAD3/4-dependent mechanism that prevents transcriptional activity [58]. Loss of TGFβ signaling is a common occurrence during the later stages of colon cancer progression and metastasis. This event may contribute to elevation of *Ptp4a3* gene expression, which may contribute to the invasiveness and metastatic potential of late-stage tumors.

The transcription factor Snail is also a direct activator of *Ptp4a3* gene transcription in SW480 colorectal cells [60]. Regulation by Snail in these cells supports a model in which *Ptp4a3* facilitates epithelial to mesenchymal transition (EMT), an important step in metastasis [61]. Additionally, expression of *Ptp4a3* in human myeloma cells lines is increased following stimulation with the cytokines IL-6 and IL-21 [15]. The mechanism by which cytokine stimulation contributes to *Ptp4a3* expression is not known. While this finding could have implications for other cell and tissue types, the extent of control over *Ptp4a3* gene expression that cytokines exhibit is not well characterized.

It is important to note that *Ptp4a3* gene activity can be further controlled through translational repression by the RNA binding protein polyC-RNA-binding protein 1 (PCBP1) [62]. Following gene expression, the *Ptp4a3* mRNA transcript contains a large 5’ untranslated

region containing several GCCCAG motifs. The PCBP1 protein binds these motifs and prevents translation of the gene product [63]. While it is not known how functionally relevant this mechanism is, PTP4A3 protein levels are inversely correlated with PCBP1 levels in several cancer cell lines.

1.4.3 Signaling mechanisms of PTP4A3

The oncogenic effects of PTP4A3 gene activity are implicated in the enhancement of many cellular phenotypes contributing to malignancy including proliferation, migration, invasion, and survival. In human tumors, high expression of PTP4A3 is associated with tumor growth and metastatic potential [36, 40, 49, 64]. The results of experimentally manipulating PTP4A3 expression in cancer cell lines, generally by the introduction of a transgene, support a functional role in cancer progression, although the mechanism by which this occurs is not well understood.

Ectopic overexpression of PTP4A3 in HEK293 cells increases SRC activation along with cell proliferation and invasion [65]. Activation of SRC function by PTP4A3 is attributable to translational control of c-SRC tyrosine kinase (CSK) [66]. The decrease in CSK protein levels, a negative regulator of SRC, corresponds to an increase in the phosphorylation of elongation initiation factor 2 (eIF2). Furthermore, activity of the distal SRC targets ERK1/2, STAT3, and p130Cas is elevated as the result of PTP4A3 overexpression in these cells [65].

Ectopic PTP4A3 overexpression increases the levels of active RhoA and RhoC in SW480 colorectal carcinoma cells [17]. In the same cells, Rac is decreased and Cdc42 is unaffected by exogenous PTP4A3 expression. While ectopic PTP4A3 expression results in increased migration and invasion, this can be reversed by the pharmacological inhibition of Rho Kinase (ROCK)

[67]. Similarly, silencing of *Ptp4a3* expression in A549 lung cancer cells decreases the levels of active RhoA and mDia1, which also lends to decreases in cellular migration and invasion [68].

PTP4A3 may contribute to cellular invasion through another mechanism: matrix metalloproteinase (MMP) activity. The MMP enzymes contribute to degradation of the extracellular matrix, which is a precursor to cell invasion and metastasis. Expression of PTP4A3 is correlated with high MMP2 and MMP9 levels in both late stage glioma [30] and hepatocellular carcinoma [43]. PTP4A3-mediated invasion in LoVo colon cancer cells is associated with upregulation of MMP2 [69]. Overexpression of PTP4A3 in DLD-1 colorectal cancer cells results in enhancement of MMP2, MMP7, MMP13, and MMP14 [70]. The invasion of these cells in a mouse model of experimental metastasis is completely dependent on the activity of MMP7 [70].

PTP4A3 overexpression in CHO cells reduces paxillin and vinculin levels at focal adhesion complexes [71]. These cytoskeletal proteins are necessary to regulate focal adhesion complex activity and actin dynamics during cell migration. The phenotype associated with PTP4A3 expression is linked to EMT – an important early step in the initiation of the metastatic cascade. PTP4A3 expression also increases the levels of active AKT while inactivating GSK3β and downregulating PTEN in DLD-1 colorectal cancer cells [71]. Treatment of cells with the phosphoinositide 3-kinase (PI3K) inhibitor LY294002 is able to mitigate EMT in PTP4A3 overexpressing cells, suggesting that PTP4A3 induced EMT requires the PI3K/AKT pathway. Modification of the AKT pathway is the most commonly reported downstream target of PTP4A3 expression in cells [16, 58, 62, 70, 71]. This may be due to the position of AKT as a central signaling molecule that feeds into a multitude of peripheral pathways rather than a direct effect on AKT itself.

It is important to note the limitations inherent in the overexpression studies that have formed the basis of what is currently known about PTP4A3. Specifically, ectopic overexpression often leads to supra-physiological levels of gene expression that are neither biologically or pathologically relevant, which can result in artifacts that may not be biologically relevant. Gene silencing can be more physiologically informative, but knockdown experiments are also subject to treatment effects as well as inefficiency and high variability. Loss of protein experiments (i.e., knockout) use genetic engineering to overcome the inconsistency and treatment-associated effects common with biochemical gene knockdown.

1.4.4 Proposed substrates of PTP4A3

While extensive effort has been put forth towards characterizing the signaling pathways modified by PTP4A3 expression, the specific macromolecules through which PTP4A3 creates these effects have remained elusive. The phosphatase assignment for PTP4A3 is based on its characteristic PTP domain, which structurally would appear to emulate the shallow binding pocket often seen in classical dual-specificity phosphatases, which are capable of dephosphorylating the shorter side chains of serine and threonine residues [20]. There is currently no published crystal structure for PTP4A3.

The cytoskeletal linker protein ezrin is proposed to be a direct substrate of PTP4A3, with phospho-threonine as the preferred catalytic target [72]. Dephosphorylation of ezrin by PTP4A3 can be observed *in vitro*, although the report described here uses whole cell lysates rather than the purified phosphatase, which leaves the potential for unknown intermediary steps. This is an attractive potential substrate because of the known role of ezrin in regulating the actin cytoskeleton, which is well established as important in cell migration. When phosphorylated,

ezrin adopts an open and active conformation, which connects various membrane components with the actin cytoskeleton [73]. Upon dephosphorylation, the protein adopts a closed conformation as the result of internal binding. The cycling of ezrin between active and inactive states is important for the regulation of cytoskeletal dynamics and cell morphology necessary for the metastatic phenotype of cancer cells [74]. Ectopic expression of PTP4A3 is associated with dephosphorylation of ezrin at Thr567 in HCT116 colorectal cancer and endothelial cells [72].

Other potential PTP4A3 substrates are the integrin receptors, a group of transmembrane proteins involved in cell adhesion and signal transduction. PTP4A3 is reported to directly interact with integrin α1 as demonstrated through cell-based assays, although the significance of this interaction is not well established [75]. PTP4A3 also directly interacts with the ADP-ribosylation factor 1 (Arf1) in endosomal compartments, which results in recycling of integrin α5 [76]. PTP4A3 binds to integrin β1, which can be enhanced by silencing of integrin α1 [76]. This interaction is associated with decreased phosphorylation of integrin β1 at Tyr783 and is dependent of PTP4A3 catalytic activity suggesting a possible direct substrate.

Two additional proteins that are associated with cell cycle progression in colorectal cancer have been identified as potential PTP4A3 substrates. Nucleolin primarily localizes to the nucleolus where it is involved in the synthesis and maturation of ribosomes. In addition to the ability to interact with nucleolin, PTP4A3 expression results in reduced nucleolin phosphorylation [77]. While a direct substrate role is not well established, high PTP4A3 levels are correlated with nucleolar expression of nucleolin in colorectal cancer. Stathmin is an oncogene that regulates microtubule remodeling and mitotic spindle assembly in proliferating cells. PTP4A3 binds to stathmin as demonstrated by co-immunoprecipitation, and this interaction

appears to contribute to microtubule destabilization in cells [78]. There is no direct evidence, however, supporting stathmin as a substrate for PTP4A3.

There also is evidence indicating PTP4A3 could be a lipid phosphatase capable of dephosphorylating phospho-inositides [79]. Recombinant PTP4A3 assayed *in vitro* demonstrates activity as a phosphatidylinositol 5-phosphatase with $PI(4,5)P_2$ being the preferred substrate. Mutation of the catalytic cysteine to serine (C104S) prevents this activity as well as the corresponding increase in cell migration. The conclusion that PTP4A3 is a phosphatidylinositol 5-phosphatase is further strengthened by the finding that PTP4A3 shares significant homology with PTEN [20], which is a known lipid phosphatase. The capacity to dephosphorylate a secondary messenger, such as phosphatidylinositol, could also explain the convolution of downstream effectors that have been previously reported.

1.4.5 Pharmacological inhibition of PTP4A3

Since the discovery of its overexpression in cancer, several small molecule inhibitors of PTP4A3 have been identified and used experimentally. The antiprotozoal compound pentamidine (Fig. 4A) inhibits the phosphatase activity of all three PTP4A family members *in vitro* albeit with low specificity and potency [80]. Pentamidine treatment suppresses proliferation of cancer cell lines known to express PTP4A genes when tested at therapeutically relevant and well-tolerated doses. However, the full mechanism of pentamidine action is not well understood and the potential exists for multiple cellular targets including other phosphatases.

A highly selective and potent reversible pan-PTP4A inhibitor, thienopyridone (7-amino-2-phenyl-5H-thieno[3,2-c]pyridin-4-one), has been reported from a high-throughput screening campaign of the Roche chemical library via fluorescence polarization assay (Fig. 4B) [81]. It

inhibits all three PTP4A proteins with IC_{50} values in the 100-300 nM range (PTP4A3 IC_{50}=128 nM) [81]. This compound exhibits minimal activity when tested *in vitro* against a panel of 11 other phosphatases, suggesting very high specificity. Furthermore, thienopyridone is able to inhibit anchorage independent cell growth of RKO and HT-29 colorectal cancer cells grown in soft agar, through a mechanism involving cleavage of p130Cas. Unfortunately, these results have not been reproduced to date nor have we been able to reproduce them (unpublished data).

Another potent small molecule inhibitor of PTP4A3 catalytic activity is BR-1 (Fig. 4C), a benzylidene rhodanine derivative, which has a reported *in vitro* IC_{50} of 0.9 µM [82]. The BR-1 compound is able to effectively inhibit the invasion of B16F10 mouse melanoma cells, which express high levels of endogenous PTP4A3 relative to the noninvasive parental cell line B16F0.

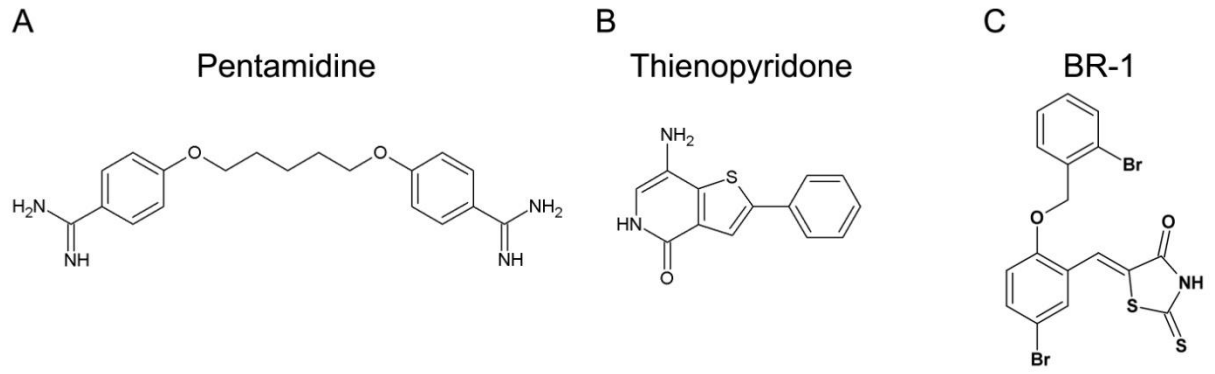

Figure 4. Small molecule inhibitors of PTP4A3

A) Pentamidine is a nonspecific pan-PTP4A inhibitor with low potency. B) Thienopyridone is another pan-PTP4A inhibitor that is highly potent and considered specific for PTP4A family members. Thienopyridone inhibits PTP4A3 with an *in vitro* IC_{50} of 128 nM. C) BR-1 is a PTP4A3 inhibitor with an *in vitro* IC_{50} of 0.9 µM.

An alternative to catalytic inhibition of enzymatic activity is interference with *Ptp4a3* gene expression. The natural product curcumin, which is known to have anti-cancer properties, is able to downregulate *Ptp4a3* mRNA in several cancer cell lines [83]. Curcumin also inhibits the growth and adhesion of B16BL6 mouse melanoma cells; and this effect is reduced upon silencing of *Ptp4a3* in cells. Although this finding suggests that inhibition of *Ptp4a3* gene transcription may be important in the anti-cancer activity of curcumin, it is likely to have many other targets in cancer cells.

Yet another method of therapeutically targeting PTP4A proteins is through the use of biological inhibitors or specific antibodies. Injectable antibodies against intracellular PTP4A1 and PTP4A3 are able to prevent experimental metastases when mice are injected with cancer cells that are expressing high PTP4A3 [84]. While this method is traditionally limited to targets on the cell surface, several studies demonstrate potential for targeting intracellular PTP4A3 protein using antibody technology [85]. In this system, host B cells are thought to participate in antibody internalization thereby exposing the therapeutic to its antigen [86].

In practice, the effectiveness of antibodies against intracellular cancer targets may not be the result of inhibiting oncogenic proteins but rather identifying malignant cells that would otherwise evade immunosurveillance and priming them for destruction by natural killer cells [85]. Because this methodology is extremely novel and not well-understood, additional information will be required before these reagents are used therapeutically and should be used with caution experimentally. Moreover, as mentioned above, the specificity of anti-PTP4A3 antibodies remains uncertain.

1.5 HYPOTHESIS AND SPECIFIC AIMS

PTP4A3 is strongly implicated in the biological events driving malignancy, yet little is known about its *in vivo* functions. Most of our knowledge regarding the role of PTP4A3 in cancer is derived from observations of patient clinical samples or distal signaling effects resulting from PTP4A3 expression or silencing in cell culture models. There are important unanswered questions as to whether PTP4A3 actually mediates the *in vivo* cancer phenotype and whether there is value in targeting PTP4A3 therapeutically.

I have developed the hypothesis that PTP4A3 gene activity facilitates *in vivo* cellular proliferation and invasion necessary for the malignant phenotype. To test this hypothesis, I developed two specific aims: 1) establish a functional contribution of PTP4A3 to the induction and progression of an animal model of colorectal cancer; and 2) determine the mechanism of PTP4A3 mediated vascular cell invasion and angiogenesis. These goals are designed to both definitively demonstrate the multilevel contribution of PTP4A3 to malignancy and establish the value of PTP4A3 as a therapeutic target *in vivo*.

2.0 CREATION AND PHENOTYPE OF PTP4A3 KNOCKOUT MICE

2.1 INTRODUCTION

PTP4A3 is strongly associated with the malignant phenotype of human cancer and may have a causal role in cancer progression. Extensive effort has been put forth to determine to biological function of PTP4A3 in cells because of its strong potential as a therapeutic target. Unfortunately, the *in vivo* properties of this phosphatase have remained poorly understood. Most PTP4A3 characterization efforts reported to date use ectopic overexpression [65], which has significant limitations, or gene knockdown in cultured tumor cell models [37] to determine downstream signaling effectors. Very little has been done to examine the role of endogenous PTP4A3 in non-malignant cells, and there is a clear lack of well-characterized animal models in the field.

High conservation of PTP4A genes throughout all mammalian species suggests necessary and non-redundant biological roles for each of the PTP4A gene products. The PTP4A proteins are also very similar is amino acid composition (the mouse and human PTP4A3 homologs are 96% identical). These observations suggest that PTP4A3 likely performs similar functions in mouse and human cells, which makes mice an ideal model organism to study the function of PTP4A3 in biological systems.

Genetically engineered animal models are an extremely valuable resource for studying gene function and determining the importance of genes for *in vivo* phenotypes. This dissertation

details the creation of a *Ptp4a3* gene targeted mouse model allowing for the global or tissue specific deletion of the functional gene product. The Cre-lox system of site specific recombination was used to delete a portion of the *Ptp4a3* gene locus which is predicted to result in a knockout allele. More information about the function of PTP4A3 in animals can provide additional insight regarding its role in other processes such as cancer.

Mice in which *Ptp4a3* was globally deleted, exhibited a grossly normal appearance no not outward signs of ill-health when examined under standard conditions. *Ptp4a3*-null tissues were histologically normal and did not show evidence of abnormal pathology. Wildtype and *Ptp4a3*-null mice had similar serum metabolite levels and no significant difference between genotypes was observed in glucose tolerance. However, fewer homozygous-null males were observed at weaning and they maintained a slightly decreased body mass. The etiology of this phenotype is not immediately obvious, although it suggests that PTP4A3 may have a necessary function in a hormone regulated process early in development.

These observations lead to the conclusion that mice without functional PTP4A3 do not have an overt phenotype, although male homozygous-null mice may have a pre-natal survival disadvantage. This is fortunate because it will allow for the examination of adult *Ptp4a3*-null mice in disease models without having to control for confounding variables. The specific goal of this thesis project is to analyze the contribution of PTP4A3 to the *in vivo* phenotype of cancer from a systems biological approach.

2.2 MATERIALS AND METHODS

2.2.1 Gene-targeting vector construction

A gene-targeting construct was created by a highly efficient recombineering method previously described [87]. Briefly, a 9.47 kb fragment of murine strain 129/X1 genomic DNA was retrieved from a bacterial artificial chromosome (clone bMQ-352O7; The Sanger Institute). The newly created targeting vector was transformed into *E. coli* and all cloning and recombination steps were performed as described in bacteria. Recombination of homologous sequences was facilitated by heat shock induction at 42°C of the lambda phage genes exo, beta and gam [88]. The activity of these genes facilitated the recombination of short homologous sequence that allowed for insertion of specific mutations.

2.2.2 Transfection of targeting vector into ES cells

R1 embryonic stem (ES) cells were grown in knockout DMEM (Invitrogen) containing 20% FBS (Invitrogen), L-glutamine (Gibco), ESGRO (Leukemia Inducing Factor) (Millipore), and β-mercaptoethanol as previously described [89]. R1 ES cells were grown on a confluent mouse embryonic fibroblast (MEF) feeder layer that was created from embryos (E14.5) containing a neomycin resistance gene and growth arrested by treatment with mitomycin-C (Invitrogen) for 3 hours. The gene targeting vector was prepared by cesium/chloride purification to ensure high quality DNA. Prior to transfection the construct was linearized by digestion with NotI. Linearized DNA (20 ug) was added to R1 ES cells in suspension and transfected by electroporation (250V charging voltage; 500V capacitance and resistance; 50 µF capacitance

timing; 360 ohms resistance timing). Cells were then plated in P100 dishes seeded with a MEF feeder layer and cultured in selection medium containing G418 (0.2 mg/mL) and gancyclovir (2.0 μM) for one week. Drug resistant clones were isolated and expanded for analysis.

2.2.3 Genotyping by Southern blot analysis

ES cell clones and mutant mice were genotyped by Southern blot of genomic DNA samples prepared by lysis and digestion with proteinase K (Sigma) as previously described [90]. Briefly, restriction digested genomic DNA was separated by gel electrophoresis (1% agarose in 4X Hellings buffer). Gels were transferred to nylon membranes (Amersham) at room temperature overnight. DNA was UV-crosslinked to the membrane and blocking was performed with prehybridization buffer containing salmon sperm DNA (0.1 mg/mL). A probe corresponding to 300 bp of exon 6 was amplified by PCR and radiolabeled with dCTP(^{32}P) with a DNA labeling kit (Roche). Hybridization was performed at 42°C overnight, and autoradiography was performed by exposing the labeled membrane to film at -80°C.

2.2.4 Quantitative RT-PCR

Total RNA was extracted from cells and tissue using Trizol reagent as per the manufacturer's protocol (Invitrogen). A total of 500 ng of RNA was converted to cDNA using the iScript first strand synthesis kit (Bio-Rad). The primers (Table 2) used for target amplification were diluted to a final concentration of 500 pM, and real-time monitoring of the PCR reaction was performed on a Biorad iQ5 thermocycler with 2X Sybr Green Mastermix (Bio-Rad). The following program was run for 40 cycles: 95°C for 0:30; 58°C for 1:00; and 72°C for 0:30.

Table 2. Primers sequences used for quantitative RT-PCR

Target Gene	Forward Sequence	Reverse Sequence	Product Size
Ptp4a1	CAACCAATGCGACCTTAA	CAATGGCATCAGGCACCC	472
Ptp4a2	ATTTGCCATAATGAACCG	ACAGGAGCCCTTCCCAAT	339
Ptp4a3	CTTCCTCATCACCCACAACC	TACATGACGCAGCATCTGG	468
Gapdh	AACGACCCCTTCATTGAC	TCCACGACATACTCAGCAC	191

2.2.5 Western blot analysis

Cells and tissues were lysed using radioimmunoprecipitation (RIPA) buffer and quantified by Bradford assay. A total protein sample of 40 µg was separated using Novex SDS-PAGE reagents (Invitrogen) and transferred to nitrocellulose membranes. Membranes were blocked in Odyssey buffer (LI-COR Biosciences) and incubated with primary antibodies overnight followed by secondary fluorescent antibodies according to the manufacturers' instructions. Commercially available primary antibodies PTP4A3 clone 318 (Santa Cruz Biotechnology) and GAPDH (Cell Signaling Technology) were used for analysis.

2.2.6 Body weight and BMI analysis

Wildtype and *Ptp4a3*-null mice, age and gender matched littermates (n=9/gender and genotype), were weighed at 6 weeks of age. Mice were also measured from the nose to the base of the tail and body mass index was determined (BMI=kg/m^2).

2.2.7 Histological comparison

Mouse tissues were isolated and submerged in 10% neutral buffered formalin (Sigma) overnight. Tissues were then submerged in 70% ethanol and transferred to the Starzl Transplant Institute Research Histology Services core facility for processing. Briefly, samples were dehydrated through an ethanol gradient, embedded in paraffin and sectioned onto glass microscope slides. Tissue sections were deparaffinized and stained with hematoxylin and eosin. Stained slides tissue sections were imaged with a bright field microscope.

2.2.8 Serum metabolite level assay

Whole blood (1.0 mL) from mice anesthetized with isoflurane was collected by cardiac puncture using an 18-gauge needle and stored on ice. Serum was purified using serum separator tubes (BD Biosciences) and samples were frozen and shipped on dry ice to Charles River Laboratories clinical pathology services for analysis of metabolite levels.

2.2.9 Glucose tolerance test

Wildtype and *Ptp4a3*-null mice (n=5/genotype, male, 6-8 weeks) were fasted overnight and challenged with D-glucose (2.0 mg/kg) via intraperitoneal (IP) injection. Blood glucose levels were measured in blood drawn from the tail vein with a Onetouch glucose monitor (LifeScan) at indicated time points for 2 hours after injection.

2.3 TARGETING STRATEGY AND VECTOR CONSTRUCTION

The Cre-lox system of site-specific recombination allows for the deletion of a targeted gene sequence following expression of the enzyme Cre recombinase in a cell [88]. Flanking all or part of a gene with loxP sites (also known as floxing) allows for Cre to recombine the sequence between the loxP sites leaving a single loxP. Introduction of this system into mice also allows for the global, temporal, or tissue-specific deletion of the target gene by genetically controlling Cre expression [91, 92].

The *Ptp4a3* gene is located on chromosome 15 in the region E1 of the mouse genome, where it consists of 6 exons spanning 8.85 kb. When the *Ptp4a3* gene is transcribed, an mRNA transcript of 1720 bp is produced. Exon 1 and the majority of the exons 2 and 6 are noncoding sequences of the transcript, with the initiation codon residing in exon 2. Thus, exon 2 was targeted for deletion to knockout the *Ptp4a3* gene (Fig. 5). The mutant *Ptp4a3* mRNA transcript lacking exon 2 will have an incorrect translational start site that is out of frame. This mutation was predicted to result in a completely nonfunctional peptide with no homology to the wildtype PTP4A3 protein.

Recombineering (recombination-mediated genetic engineering) is a fast and efficient method of manipulating genetic material in *E. coli* [87] and was utilized in construction of the *Ptp4a3* gene-targeting vector. A bacterial artificial chromosome (BAC) containing Strain 129X1 mouse genomic DNA (The Sanger Institute) was used to obtain the starting material for construction of the gene-targeting vector. Retrieval of a wildtype gene fragment containing exons 1 through 5 of the *Ptp4a3* locus was performed by inserting short homologous sequences corresponding to each end of the target sequence into the pLi-PGKtk cloning plasmid. Homologous sequences were recombined with the BAC DNA in bacterial cells that resulted in

retrieval of a wildtype fragment (9.47 kb) containing exons 1 through 5 of the mouse *Ptp4a3* gene (Fig. 5A).

A neomycin resistance cassette (NEO) [87] surrounded by loxP sites was inserted into intron 1 as the first step in targeting exon 2 for deletion (Fig. 5B). The targeting vector was transfected into cells with an inducible Cre recombinase. Following Cre expression, the floxed neomycin cassette was recombined leaving a single loxP site (Fig. 5C). Finally, a NEO cassette flanked with FRT sites adjacent to a single loxP site was inserted into intron 2 (Fig. 5D). This was the targeting vector that was used for transfection into mouse ES cells. Sequencing of the targeting vector was performed to exclude the possibility of confounding mutations in the floxed allele.

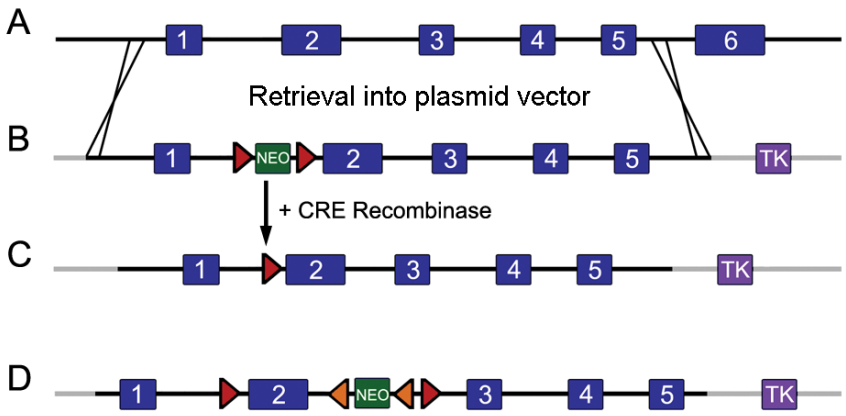

Figure 5. Targeting vector constructed for *Ptp4a3* mutation

A) Genomic DNA corresponding to the *Ptp4a3* locus was cloned into a vector containing thymidine kinase (purple) by homologous recombination in *E coli*. B) Insertion of a NEO cassette (green) surrounded by loxP sites (red arrows) is the first targeting step and allows for selection when transformed into cells. C) Recombination caused by expression of Cre recombinase left a single loxP site adjacent to exon 2. D) Insertion of a NEO cassette surrounded by FRT sites (orange arrows) adjacent to a single loxP site completed that targeted mutation that was recombined into the mouse genome.

2.4 GENE-TARGETING IN EMBRYONIC STEM CELLS AND CHIMERIC ANIMAL PRODUCTION

The mutatant targeting vector was confirmed by nucleotide sequencing and transfected into the R1 ES cell line (Strain 129X1/SvJ) [89] and grown with MEF feeder layer. Following transfection, the cells were cultured with G418 (geneticin) and gancyclovir for positive and negative selection of correctly targeted clones [93]. Homologous recombination of the NEO cassette was necessary for resistance to G418, while loss of the active thymidine kinase was necessary for resistance to gancyclovir (Fig. 6A). This strategy selects against cells not transfected as well as random integration events.

ES cell clones were genotyped by Southern blot analysis with HindIII as the primary screening assay (Fig. 6B). A radiolabeled external probe, comprising approximately 300 bp corresponding to exon 6 of the *Ptp4a3* locus, was used to detect the targeted mutation. A high targeting efficiency was achieved with 44 out of 76 tested clones being identified as correctly targeted as evidenced by the presence of a 10.2 kb band (Fig. 6B).

Correct targeting was confirmed with additional Southern blot assays based on the expected and observed restriction fragment sizes (Fig. 6A). Detection was performed with PCR amplified 5' and 3' probes that were external to the targeting vector. Each of the 3 tested enzymes (BamHI, HindIII and BglII) produced different fragment sizes based on genotype. Two correctly targeted cell clones (identified as 207-3E6 and 214-1A6) that produced the expected band sizes with multiple digests were chosen for expansion and injection into blastocysts for chimeric mouse production.

Cells heterozygous for the $Flox_{NEO}$ allele were injected into day 3.5 postcoitum mouse embryos from C57BL/6J mice. Pseudo-pregnant CD-1 female mice (mated to vasectomized CD-

1 males) were injected with 7-8 chimeric embryos in each uterine horn. These procedures were primarily performed by Carolyn Ferguson (University of Pittsburgh, Department of Anesthesiology). Implanted blastocysts were allowed to come to term and the resulting offspring were derived from both targeted R1 stem cells and the endogenous C57BL/6J blastocysts. Clone 207-3E6 produced chimeric mice (n=4) that were derived from both C57BL/6J and 129X1/SvJ ES cells, as evidenced by mixed black and agouti coat color. These mice were mated to C57BL/6J females and a portion of the resulting offspring was heterozygous for the mutant allele, which confirmed germline transmission of the targeted allele for all 4 chimeric mice.

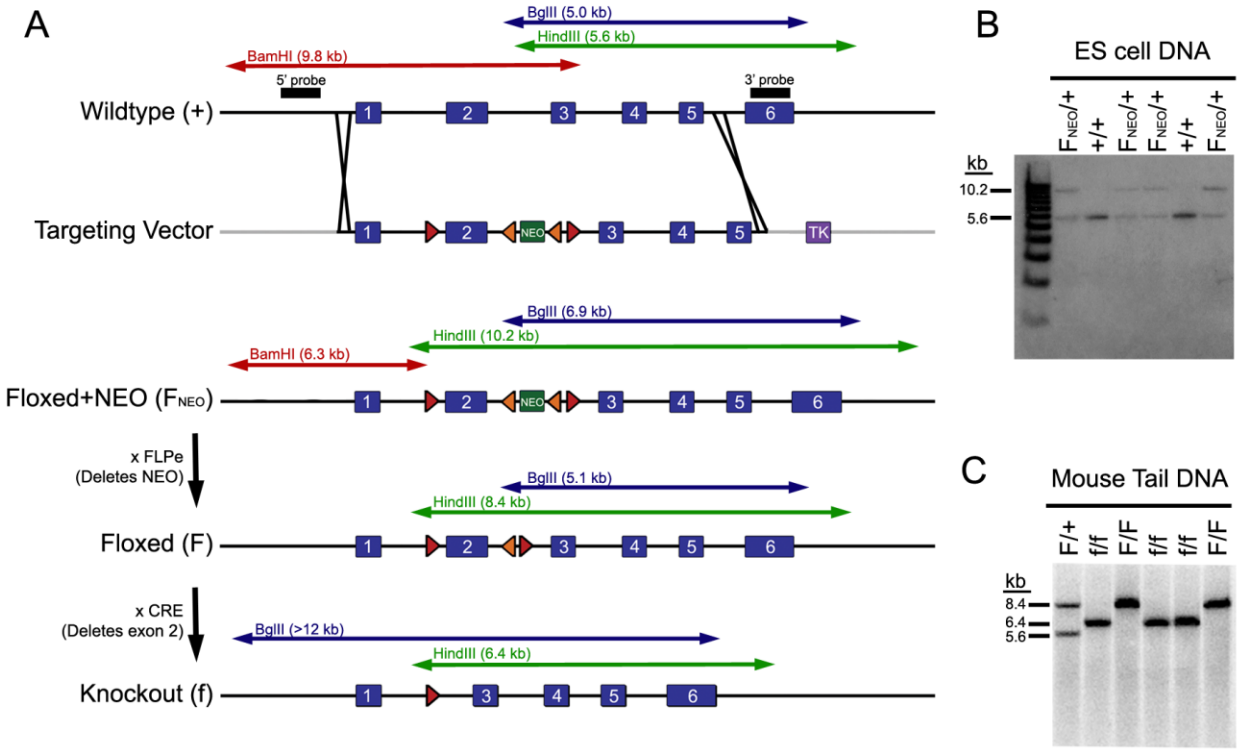

Figure 6. Strategy developed for gene-targeting the mouse *Ptp4a3* locus

A) Transfection of the gene targeting vector into mouse ES cells was followed by homologous recombination into the genome with the wildtype *Ptp4a3* locus. Genomic DNA was restriction digested with multiple enzymes and Southern blot performed with multiple probes to confirm correct recombination of the targeted allele in ES cells. Each of the above enzymes (BamHI, HindIII and BglII) produces different fragment sizes from wildtype compared to targeted

($Flox_{NEO}$) sequences. Targeted mice were crossed to a transgenic strain expressing FLPe recombinase from a general promoter (β-actin). FLPe recombined the FRT sites to remove the NEO cassette creating the floxed allele. Floxed mice were then crossed to a transgenic strain expressing Cre recombinase from a general promoter (EIIA). Cre recombined the loxP sites to delete exon 2 and create the knockout allele. B) Genomic DNA isolated from ES cell clones was restriction digested with HindIII and Southern blot performed with an exon 6 probe. The wildtype restriction fragment was 5.6 kb in length while insertion of the loxP and NEO sequences results in a 10.2 kb fragment. The clones assayed in lanes 1, 3, 4, and 6 are heterozygous for the targeted mutation; lanes 2 and 5 homozygous for the wildtype allele. C) Southern blot analysis of genomic DNA was used to monitor these genetic changes and genotype mice containing the wildtype, floxed, or knockout alleles.

The newly established *Ptp4a3* mutant mouse strain was mated to mice with transgenic expression of FLPe recombinase from a global β-actin promoter [94]. Following expression of FLPe, the area surrounded by FRT sites including the NEO cassette was recombined leaving a single FRT site (Fig. 6A). The resulting mutation was referred to as the floxed allele (floxed exon 2), which left the *Ptp4a3* genetic locus intact. Mutant mice were also crossed with mice expressing a Cre transgene from a global (mosaic) EIIA promoter [95]. Expression of Cre resulted in deletion of the targeted portion of the *Ptp4a3* locus that was predicted to result in a nonfunctional or knockout allele. Both transgenes were bred out of the strain through mating to C57BL/6J wildtype mice. These alleles were backcrossed to the C57BL/6J strain for a total of 5 generations and mice heterozygous for the mutant floxed and knockout alleles (F/f) were created. In knockout studies such as this, the *Ptp4a3* floxed allele is the preferable control as opposed to C57BL/6J wildtype allele [96]. This is because the in F1 generation mice, genes linked to the targeted locus are Strain 129 derived, while the corresponding wildtype locus is C57BL/6J derived. Breeding heterozygous mice (F/f) maintains the Strain 129 linked genes for all experimental animals.

2.5 PHENOTYPE OF PTP4A3 MUTANT MICE

2.5.1 Expression and localization of mouse PTP4A3

Ptp4a3 gene expression was initially thought to be restricted to heart and skeletal muscle with lower levels in the pancreas as detectable by Northern blot assay [25]. Endogenous expression of PTP4A3, particularly the protein product, has not previously been well characterized due to lack of antibody efficacy and specificity as mentioned above. The creation of homozygous-null samples provided a novel opportunity to assay PTP4A3 protein expression and account for antibody specificity with an ideal negative control. Therefore, several tissue types were assayed for PTP4A3 protein expression by Western blot (Fig. 7). Of the samples assayed, fetal heart and adult spleen appeared to express the highest level of PTP4A3 protein. Fetal intestine, adult heart, skeletal muscle, pancreas, lung, spleen, brain, thymus, colon, and small intestine all expressed detectable levels of PTP4A3 in contrast to the liver and kidney, which had no detectable PTP4A3 protein. Absence of a signal from knockout spleen lysate confirmed that the antibody detected PTP4A3 (Fig. 7).

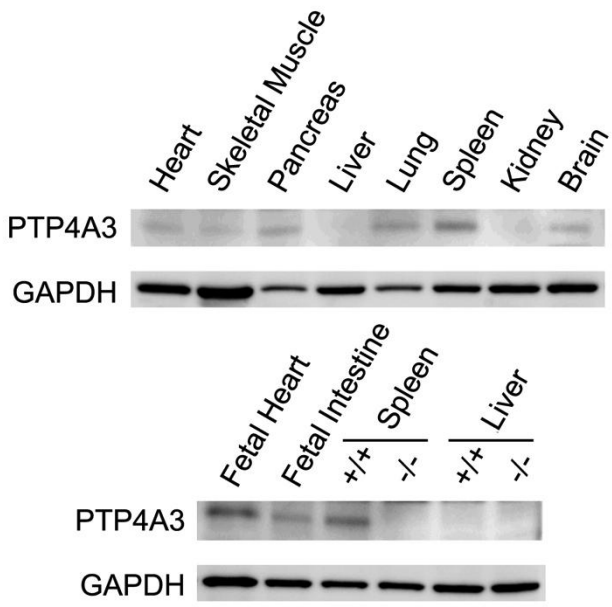

Figure 7. PTP4A3 protein was expressed in adult and fetal mouse tissues

Whole organ samples were homogenized and protein lysates were created. Tissue lysates (40µg) were assayed by Western blot for expression PTP4A3 and GAPDH (control). Most tissues expressed detectable levels of PTP4A3, except liver and kidney, which did not have PTP4A3. Antibody specificity was confirmed by absence of a signal in the homozygous knockout negative control.

The lack of specific and functional antibodies for immunohistochemical detection of PTP4A3 prevented direct examination of PTP4A3 location in the cell. To determine the localization PTP4A3 in cells, I generated a transiently expressed Green Fluorescent Protein (GFP) or GFP-tagged PTP4A3 construct in a Rat2 fibroblast cell line and examined fluorescence 24 hour after transfection (Fig. 8). As expected, GFP alone exhibited diffuse fluorescence without a discernible localization preference. The GFP-PTP4A3 protein was observed at the plasma membrane and intracellular structures (likely endomembranes). This localization pattern supports previous studies using other cell types that suggested PTP4A proteins are membrane associated [14, 16]. While association with the plasma membrane is visually obvious, additional

experiments (such as co-localization with low-density lipoprotein receptor) will be required to confirm that the intracellular localization is the result to endosomal compartments. Additionally, GFP-PTP4A3 overexpressing cells appeared to adopt a conformation that supports a role in migration.

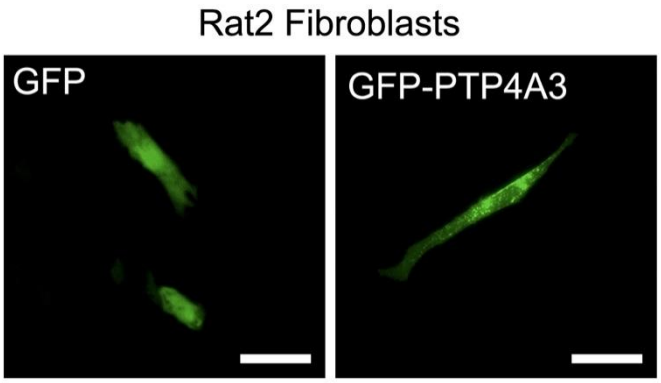

Figure 8. Cellular localization of a GFP-PTP4A3 fusion construct was membrane associated

Rat2 fibroblast cells were transiently transfected with GFP or a GFP-PTP4A3 fusion construct. GFP produced fluorescence throughout the cell, while GFP-PTP4A3 appeared to localize to the plasma membrane and endosomal structures (bar=10 μm).

2.5.2 Knockout of the PTP4A3 gene product

Because fetal heart tissue has high levels of *Ptp4a3* expression [26], quantitative RT-PCR on total RNA samples from fetal heart tissue (E19.5) was performed to determine the relative mRNA levels of *Ptp4a1*, *Ptp4a2*, and *Ptp4a3*. While *Ptp4a1* and *Ptp4a2* levels remained similar between genotypes, *Ptp4a3* mRNA was reduced in heterozygous tissue and not detectable in samples from *Ptp4a3*-null fetal heart tissue (Fig. 9A). Thus, compensation for *Ptp4a3* loss by upregulation of either family members *Ptp4a1* or *Ptp4a2* at the mRNA level was excluded.

Protein lysates from fetal heart tissue were assayed by Western blot for the presence of the PTP4A3 protein product. While detectable in samples from wildtype embryos, PTP4A3 was

lower in lysates from heterozygous embryos and homozygous-null tissue contained no detectable PTP4A3 (Fig. 9B).

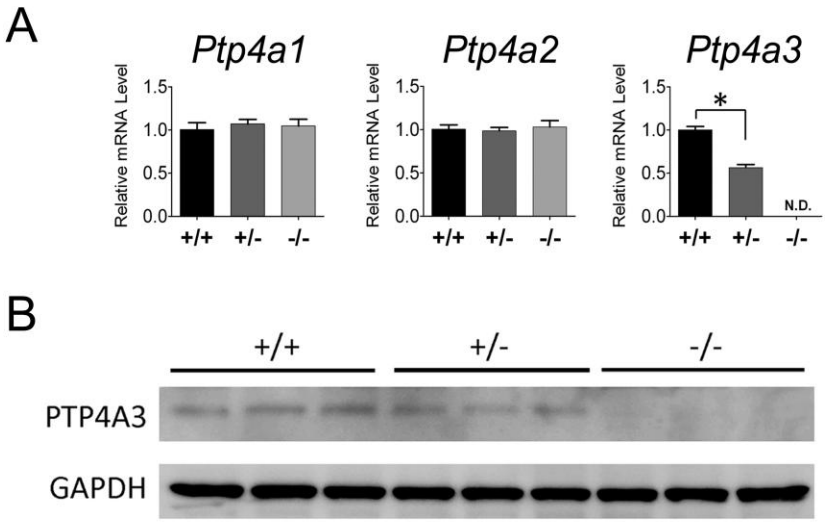

Figure 9. Gene deletion resulted in knockout of functional PTP4A3

A) Quantitative RT-PCR analysis on total mRNA from fetal heart tissue revealed no change in *Ptp4a1* and *Ptp4a2* mRNA levels while *Ptp4a3* was reduced and not detectable in heterozygous and homozygous-null tissue, respectively. B) The PTP4A3 protein product was detectable by Western blot in whole protein lysates from wildtype and heterozygous fetal heart tissue, but not in homozygous *Ptp4a3*-null samples.

2.5.3 Decreased birthrate and body mass in male *Ptp4a3* knockout mice

An analysis of >500 pups that were produced by heterozygous mating pairs indicated all potential genotypes were observed in the resulting offspring. While females were observed at the expected Mendelian ratios, there was a significant decrease in the number of *Ptp4a3*-null males at weaning relative to the predicted frequency (Table 3). Given this finding, it is possible that knockout males either possessed a survival disadvantage (either *in utero* or post-natal) or that *Ptp4a3*-null germ cells had a preconception phenotype.

Table 3. Observed genotype of mouse offspring at weaning

There was an observed decrease in number of male *Ptp4a3*-null mice observed at weaning relative to the expected amount predicted by Mendelian genetics ($p<0.05$). Female mice of each genotype were born at the expected frequency (1:2:1).

Male	+/+	+/-	-/-	**n**	χ^2	**p**
Observed	75	117	48	240	6.23	<0.05
Expected	*60*	*120*	*60*			
Female	+/+	+/-	-/-	**n**	χ^2	**p**
Observed	70	127	79	276	2.34	N.S.
Expected	*69*	*138*	*69*			

Ptp4a3-null male mice exhibited a 10% decrease in body mass (Fig. 10A) and 7% decrease in body mass index (BMI) (Fig. 10B) compared to wildtype littermates at 6 weeks of age. This phenotype also appeared to be confined to male mice as female *Ptp4a3*-null mice did not exhibit a significant decrease in body mass or body mass index.

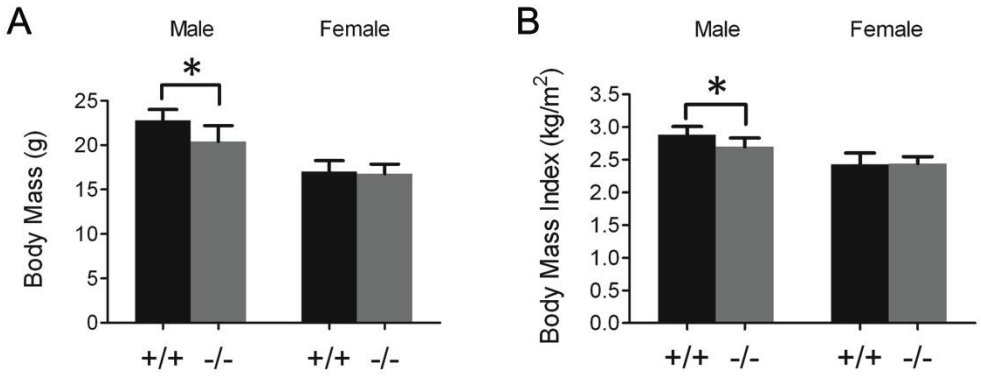

Figure 10. Reduced body mass and BMI in *Ptp4a3*-null mice

A) When compared to wildtype littermates (n=9/genotype), male *Ptp4a3*-null mice exhibited an average of 10% less body mass ($p<0.005$). B) Mice were also measured from the nose to the base of the tail and body mass index was determined (BMI=kg/m^2). Male *Ptp4a3*-null littermates exhibited a 7% decrease in BMI compared to wildtype ($p<0.005$). Neither of these phenotypes was significantly altered in female *Ptp4a3*-null mice compared to wildtype.

2.5.4 Histological profile of *Ptp4a3*-null mice

Because PTP4A3 protein was expressed in most tissue types (Fig. 9), tissue samples from wildtype and *Ptp4a3*-null mice were examined. A histological analysis was performed on wildtype and *Ptp4a3*-null tissue sections stained with hematoxylin and eosin (Fig. 11). Upon examining multiple tissue types, no overt abnormalities were observed and all samples appeared qualitatively normal. This result suggested that PTP4A3 was not required for normal murine development and *Ptp4a3* deficiency did not cause overt histopathology.

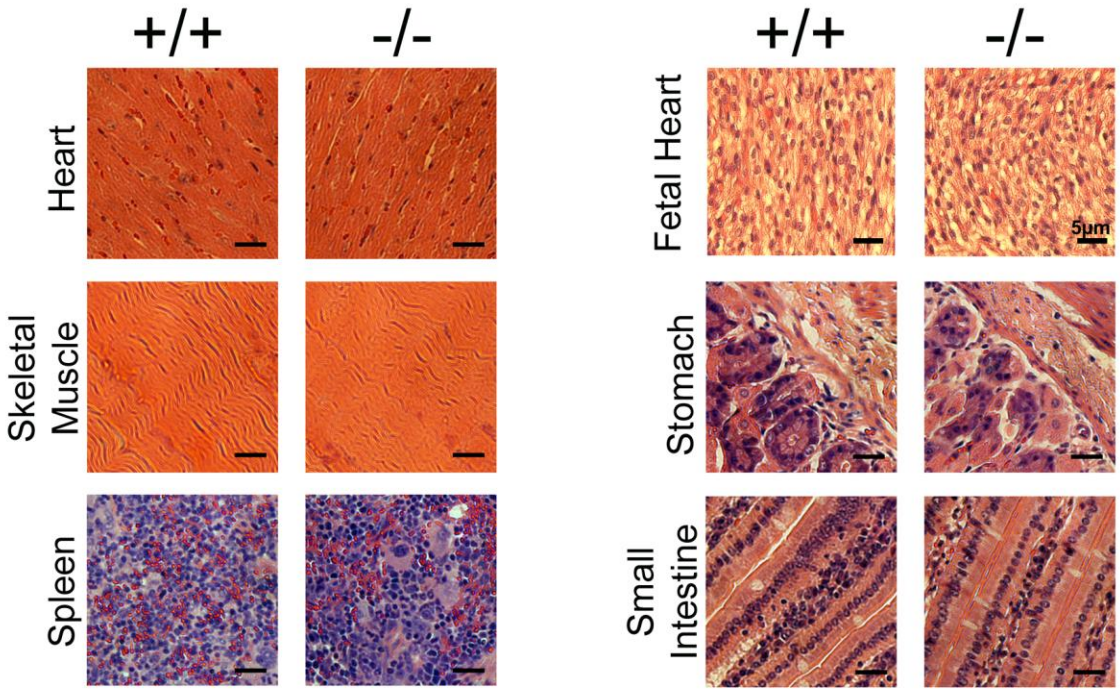

Figure 11. Histological comparison of wildtype and *Ptp4a3*-null tissue sections

Tissue sections (Fetal heart, adult heart, skeletal muscle, stomach, spleen, small intestine) from wildtype and *Ptp4a3*-null mice were compared and exhibited similar characteristics. No overt histopathology was observed in any of the samples taken from mice deficient for PTP4A3 (bar=5µm).

2.5.5 Metabolic characteristics

The potential for organ dysfunction or metabolic defects was assessed by collecting serum samples from wildtype and *Ptp4a3*-null mice. Proper liver and kidney function is required to maintain basal levels of several metabolites that are detectable in serum. None of the assayed metabolite levels exhibited a significant difference by genotype (Fig. 12). This indicates that under basal conditions *Ptp4a3*-null mice were metabolically normal and able to maintain homeostasis.

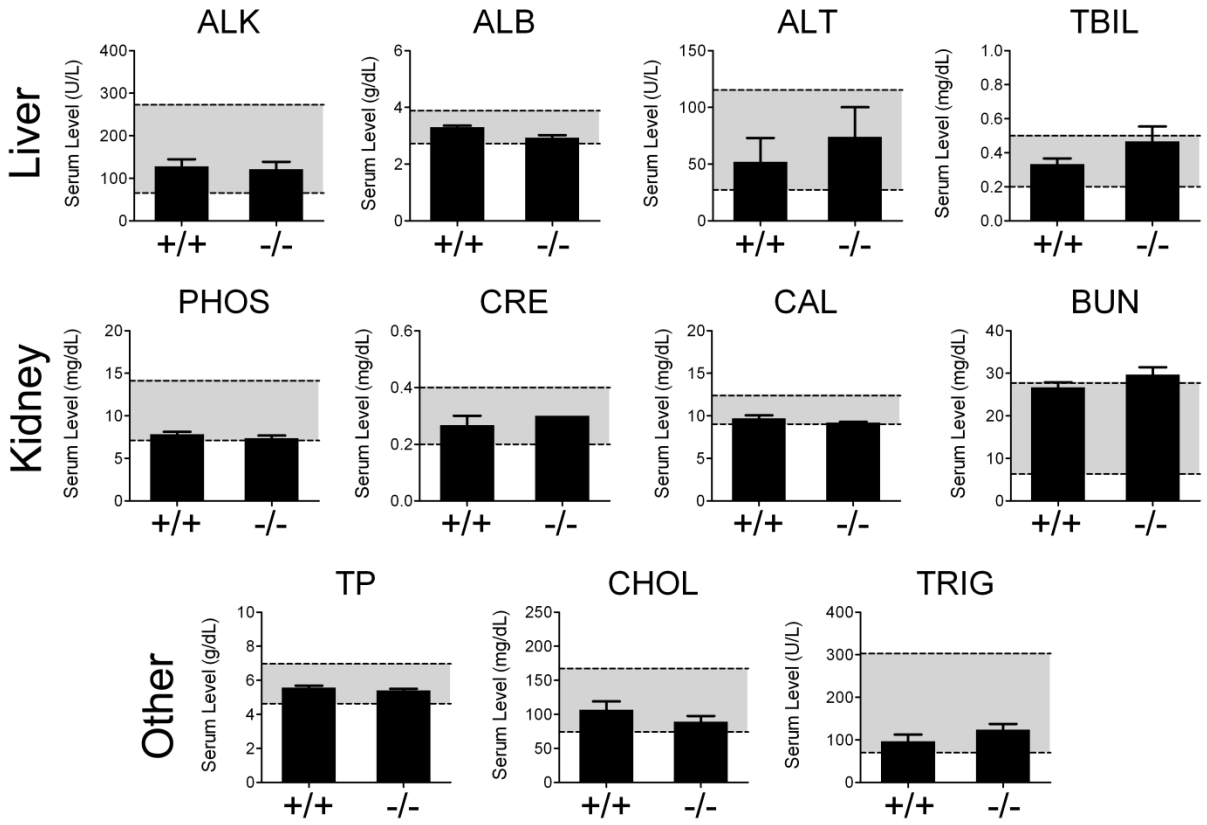

Figure 12. Serum metabolite levels in wildtype and *Ptp4a3*-null mice

Serum was collected from wildtype and *Ptp4a3*-null mice (n=3/genotype) that were fasted overnight. Several liver and kidney metabolites as well as other serum markers were assayed by Charles River Laboratories. The levels of each metabolite were not significantly different by

genotype. All except blood urea nitrogen (BUN) in *Ptp4a3*-null mice were within the normal range (shaded area) for C57BL/6J mice.

Mice were also challenged with a glucose tolerance test. Glucose homeostasis is a tightly controlled and complex process that involves the storage of blood glucose following the release of insulin from pancreatic β cells. Expression of PTP4A3 in the pancreas and skeletal muscle suggests potential involvement in this process. As indicated in Figure 13, however, no difference in glucose blood levels were seen between wildtype and *Ptp4a3*-null mice after injection with glucose.

Figure 13. Glucose tolerance in wildtype and *Ptp4a3*-null mice

Wildtype and *Ptp4a3*-null mice (n=5/genotype) that were fasted overnight and injected with D-glucose (2.0 mg/kg) via intraperitoneal (IP) injection. Blood glucose levels were measured with a LifeScan Onetouch glucose monitor at indicated time points up to 2 hours after injection. Blood glucose was not significantly different by genotype at any time point tested.

2.6 DISCUSSION

Gene targeting and ES cell technologies were used to create a *Ptp4a3* knockout mouse line. Deletion of PTP4A3 protein was confirmed by Western blot analysis using a fetal heart tissue lysates from wildtype and *Ptp4a3*-null mice. While initial studies had suggested *Ptp4a3* expression was restricted to heart, skeletal muscle, and pancreas [25], these data revealed a more ubiquitous expression pattern (Fig. 9). While the highest levels of PTP4A3 protein were observed in fetal heart, it was also detectable at lower levels in adult heart, skeletal muscle, spleen, pancreas, brain, lung, thymus, colon, and small intestine. No PTP4A3 protein was detectable the liver or kidney.

Despite the apparent importance of PTP4A3 in tumor biology, our understanding of the functionality of PTP4A3 is severely limited due in part to the absence of informative animal models. The gene targeted mouse model for disruption of the *Ptp4a3* genomic locus is useful not only for studying the phenotypic changes that occur with the global loss of the phosphatase, but also for future investigations on tissue and temporal specific gene deletion and collaborative interactions with other genes including the two other members of the *Ptp4a* family. Importantly, this model could be used to study the involvement of PTP4A3 in various cancer types that are modeled in mice. The ability to induce cell type specific knockout will add further information about the specific etiological contributions of PTP4A3 to the disease.

This model establishes that mice can survive in the absence of a functional PTP4A3 gene, although there were a slightly lower number of male mice produced, and they were able to live to maturity under normal conditions without any major health deficiencies. This is in contrast to what has been reported with mice lacking the highly homologous PTP4A2, which is thought to be the most ubiquitously expressed family member under normal conditions. *Ptp4a2*-null mice

exhibited defective placental development and both genders showed retarded growth at embryonic and adult stages [24]. PTP4A2 loss decreases the spongiotrophoblast and decidua layers of the placenta impairing nutrient transport and causing embryonic growth retardation. Moreover, loss of PTP4A2 results in AKT inactivation, which was not evident in the data regarding PTP4A3 loss. Collectively, the differences in the two gene deletion models are consistent with non-overlapping functions of these two close phosphatase family members.

The mild phenotypic differences observed in *Ptp4a3*-null mice did not indicate a strong need for PTP4A3 in the biology of developing and adult mice. This was likely the result of other genes compensating for PTP4A3 loss – possibly PTP4A1 and PTP4A2. Despite a normal histological profile, decreased body mass (Fig. 10) suggested a potential role in cell proliferation. Further research will be required to determine if there is a concrete basis for this phenotype or if this is an artifact of gene deletion. Body mass is a complex trait and it has been estimated that 31% of all viable knockout strains exhibit a significant decrease in weight [97]. It is interesting however, that females did not exhibit similar phenotypic changes. Regulation of *Ptp4a3* gene expression by sex specific hormones has not been reported, although this would provide a basis for gender specific differences. Further research will be required to shed light on the endogenous role of *Ptp4a3* as well as the male specific phenotype reported here.

3.0 DELETION OF PTP4A3 SUPPRESSES MURINE COLON CANCER

3.1 INTRODUCTION

Interest in *Ptp4a3* can be attributed to its significant potential as a biomarker and as a therapeutic target for malignant cancers. Many human cancers express high *Ptp4a3* transcript levels including tumors of the colon [8], breast [49], ovary [52], liver [43], stomach [39], and stroma [55], and elevated *Ptp4a3* gene expression often correlates with increased tumor invasiveness and poor prognosis [64]. Additionally, ectopic PTP4A3 overexpression enhances tumor cell migration and invasion *in vitro* [17]. While definitive evidence is lacking, PTP4A3 has been proposed to modulate multiple signaling pathways involving SRC [65], Rho GTPases [17], and PI3K-Akt [71] in various forms of cancer. The complexity of the pathway alterations seen when PTP4A3 is overexpressed may also reflect its ability to act as a phosphatidylinositol 5-phosphatase [79]. No reports have conclusively demonstrated a role for PTP4A3 in the physiology of normal cells or tissues.

Azoxymethane (AOM) is a procarcinogen that when metabolized in the colon is mutagenic and drives tumorigenesis [98]. The combination of AOM with the inflammatory agent dextran sodium sulfate (DSS) is a widely-used murine model that faithfully replicates colon malignancies driven by chronic inflammatory conditions such as ulcerative colitis [99]. Several signaling pathways are implicated in the pathogenesis of AOM-induced colon cancer including

KRAS [100], β-Catenin [101], c-MYC [102], Insulin-like Growth Factor-1 Receptor β (IGF1Rβ) [98], and Transforming Growth Factor β (TGFβ) [103]. Interestingly, PTP4A3 has been identified as a direct regulatory target of TGFβ signaling in colon cancer [58]. In response to TGFβ exposure, the SMAD3/4 complex inhibits transcription of the *Ptp4a3* gene in normal colon cells.

The following experiments interrogate the potential role of PTP4A3 in colon carcinogenesis using mice lacking functional PTP4A3 protein. AOM exposure acutely increased *Ptp4a3* gene expression in the colon. *Ptp4a3*-null mice were resistant to colon tumorigenesis implicating this gene in the pathogenesis of malignant disease. Moreover, tumors derived from *Ptp4a3*-null mice expressed higher levels of the cancer associated IGF1Rβ and c-MYC suggesting involvement of these oncogenic signaling pathways.

3.2 MATERIALS AND METHODS

3.2.1 Colitis-associated cancer model (AOM/DSS)

Wildtype and *Ptp4a3*-null mice (male, 6-8 weeks) were administered a single dose of AOM (12.5 mg/kg) (Sigma) in sterile saline by IP injection. DSS solution (2.5%) (MP Biomedical) was provided in the drinking water *ad libitum* for 7 days followed by 14 days of normal drinking water and this cycle was repeated a total of 3 times [99]. Experimental mice were sacrificed at 12 or 16 weeks following the initiation of treatment, at which point colon tissue was isolated, rinsed, and opened longitudinally for analysis. Tumor and normal tissues were either snap frozen in liquid nitrogen or submerged in 10% neutral buffered formalin and incubated at room

temperature overnight. For each mouse, individual tumors were counted and measured with a digital caliper and average tumor count and diameter were determined for each genotype.

3.2.2 Reverse phase protein array

Protein lysates that were made with RIPA buffer (100 μg each) from individual colon tumor samples (n=5/genotype) were denatured and shipped frozen to MD Anderson Cancer Center Functional Proteomics Core (Houston, TX) for analysis. Briefly, lysates were two-fold-serial diluted for 5 dilutions and arrayed on nitrocellulose-coated slides, probed with antibodies, and visualized by diaminobenzidine colorimetric reaction. Relative protein levels for each sample were determined by interpolation curves of each dilution curves from the standard curve antibody slide. All data points were normalized for protein loading and transformed to linear value. Linear values were transformed to $\log_2$ value and then median-centered for hierarchical cluster analysis. The heatmap was generated in Cluster 3.0 as a hierarchical cluster using Pearson Correlation and a center metric.

3.2.3 Western blot analysis

Cells and tissues were lysed using radioimmunoprecipitation (RIPA) buffer and quantified by Bradford assay. Total protein samples of 40 μg were separated using Novex SDS-PAGE reagents (Invitrogen) and transferred to nitrocellulose membranes. Membranes were blocked in Odyssey buffer (Li-COR Biosciences) and incubated with primary antibodies overnight followed by secondary fluorescent antibodies according to the manufacturers' instructions. The following commercially available primary antibodies were used: PTP4A3 clone 318 (Santa Cruz

Biotechnology), GAPDH, IGF1Rβ, c-MYC, p-AKT(S473), and AKT (Cell Signaling Technology).

3.2.4 Quantitative RT-PCR

Total RNA was extracted from cells and tissue using Trizol reagent as per the manufacturer's protocol (Invitrogen). A total of 500 ng of RNA was converted to cDNA using the iScript First Strand Synthesis kit (Bio-Rad). The primers (Table 2) used for target amplification were diluted to a final concentration of 500 pM, and real-time monitoring of the PCR reaction was performed on a Bio-Rad iQ5 thermocycler with 2X Sybr Green Mastermix (Bio-Rad). The following program was run for 40 cycles: 95°C for 0:30; 58°C for 1:00; and 72°C for 0:30.

3.2.5 Cell culture and MEF treatment

MEFs that were immortalized by infection with SV40 [104] were transfected with a chimeric c-MYC estrogen receptor (MycER) that responds to treatment with 4-hydroxytamoxifen (4-HT) [105]. Cells were cultured in DMEM containing 10% FBS (Invitrogen) in standard tissue culture flasks (BD Biosciences). 4-HT (Sigma) was solubilized in ethanol and added to medium at a final concentration of 250 ng/mL.

3.2.6 Statistics

Statistical analysis of offspring genotype was calculated by the Chi-squared test comparing observed and expected results. Data from cellular assays, Western blot, and quantitative RT-PCR

quantifications were analyzed using the 2-tailed T-test. In both cases, significance was defined as $p \leq 0.05$.

3.3 RESULTS

3.3.1 *Ptp4a3* gene expression increases immediately following AOM exposure

Since PTP4A3 protein was detectable in the normal colon epithelium (Fig. 8), *Ptp4a3* gene expression was assayed immediately following treatment with the intestinal pro-carcinogen AOM (12.5 mg/kg) or saline control in wildtype C57BL/6J mice. Mice were sacrificed 8 or 24 hours after AOM injection and colon epithelial cells were collected for analysis. Total RNA was isolated and quantitative RT-PCR was performed to assay for *Ptp4a3* gene expression levels. Interestingly, *Ptp4a3* was upregulated by 78% at 8 hours and 60 % at 24 hours in AOM-treated normal epithelial relative to control (Fig. 14A). Protein lysates from AOM treated mice suggest that the PTP4A3 protein level was also upregulated in these tissues (Fig. 14B). While the role of PTP4A3 in colon cancer is traditionally thought to involve late-stage tumors and metastasis, this finding suggested a potential role in early-stage disease and tumorigenesis.

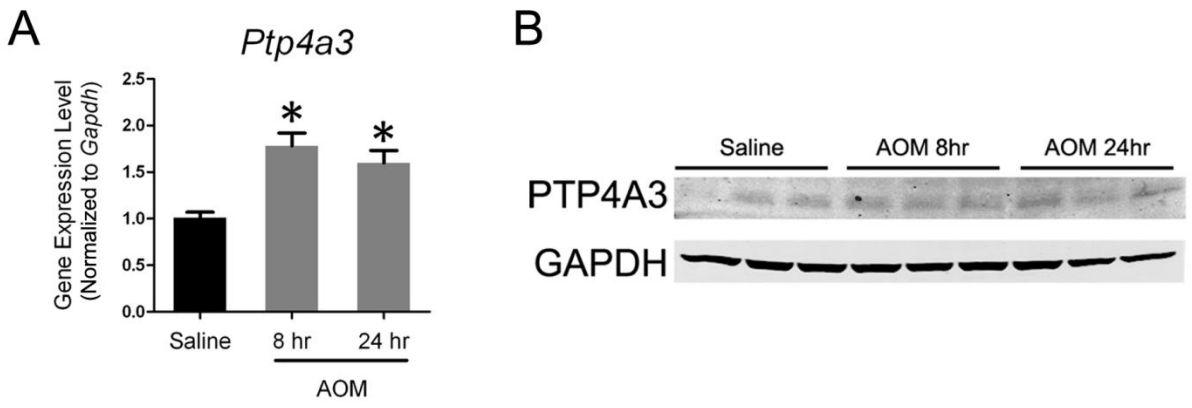

Figure 14. Elevated *Ptp4a3* expression observed in normal colon following AOM exposure

A) Quantitative RT-PCR was used to assay *Ptp4a3* gene expression in normal colon epithelial tissue following treatment with either AOM or saline control. *Ptp4a3* was elevated 73% in colon tissue when measured 8 hours after injection, and 60% at 24 hours ($p<0.001$). B) Western blot of lysates from AOM treated colon tissues demonstrates upregulation of the PTP4A3 protein following acute AOM exposure.

3.3.2 PTP4A3 is elevated in AOM-derived colon tumors

Experimental mice were treated with a widely used carcinogen-based model of colitis-associated colon cancer. Wildtype and *Ptp4a3*–null mice were injected with a single dose of AOM (12.5 mg/kg) followed by three cycles of 2.5% DSS consumption (Fig. 15A). This treatment produces distinct histological changes relative to untreated controls, including inflammation (i.e. monocyte infiltration) corresponding to DSS treatment, and subsequent dysplasia (Fig. 15B).

Because high expression of PTP4A3 has been reported in human primary colon tumors [27], *Ptp4a3* expression in the mouse model of colon cancer was examined. First, total mRNA was extracted from tumor tissue from wildtype mice and quantitative RT-PCR was used to assay for the expression level of each *Ptp4a* family member (Fig. 15C). Relative to normal colon epithelium, *Ptp4a3* was elevated 4-fold on average ($p<0.01$). While considerable heterogeneity

in *Ptp4a3* expression was observed, ranging from 1.4 to 6.7-fold upregulation, *Ptp4a3* mRNA levels in tumor tissue were consistently higher than normal tissue for every sample tested (n=15). Interestingly, the gene expression levels of *Ptp4a1* and *Ptp4a2* were both downregulated 64% and 36% ($p<0.0001$ and $p<0.05$), respectively, in colon tumors relative to normal tissue. PTP4A3 protein levels in normal colon epithelial lysates were very low when assayed by Western blotting (Fig. 15D). In contrast, PTP4A3 was readily detectable in colon tumor samples. The lack of functional antibodies for PTP4A1 and PTP4A2 precluded evaluating the tumor protein levels for these family members.

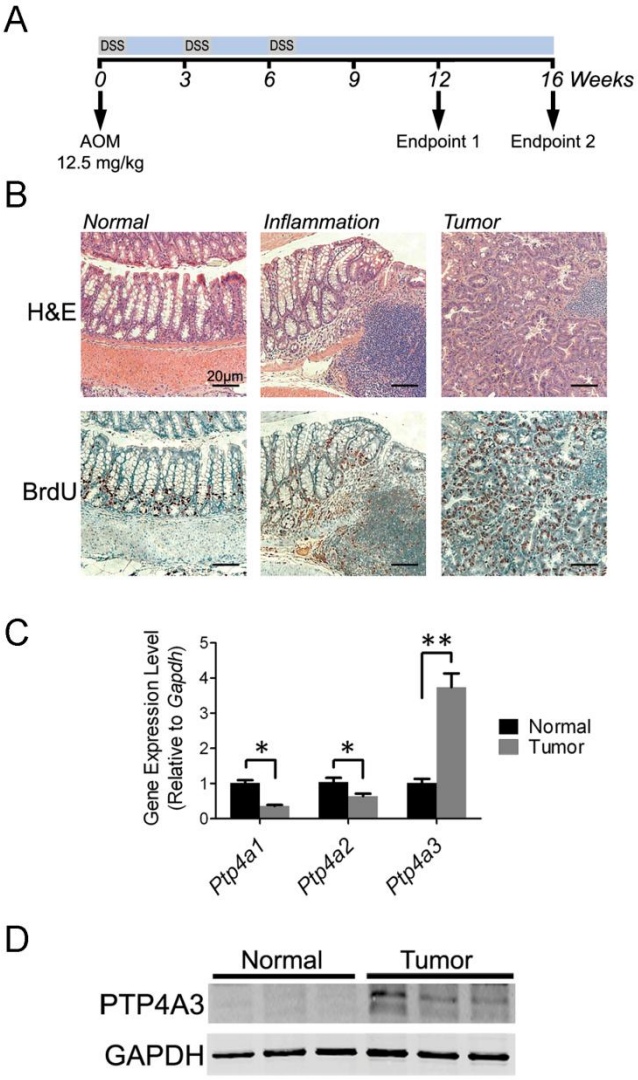

Figure 15. PTP4A3 overexpression was observed in murine colon tumors

A) The AOM-DSS treatment paradigm used in this study featured a single dose of AOM followed by 3 treatment cycles of DSS in the drinking water. B) Histological representation of normal colon tissue relative to tumor tissue demonstrated the efficacy of the AOM/DSS model. Following one cycle of DSS treatment (center panels), crypt dysplasia and mononuclear cell infiltration were apparent (lower right quadrant). Tumor tissue was present at both the 12 and 16 week endpoints. Before sacrifice, mice were treated with BrdU for 4 hours and cell proliferation was visualized by staining with a BrdU antibody. C) Quantitative RT-PCR was used to assay gene expression levels of *Ptp4a* family members in normal colon and tumor tissue. *Ptp4a3* was elevated 3.7-fold ($p<0.01$), while *Ptp4a1* and *Ptp4a2* levels were significantly decreased ($p<0.0001$ and $p<0.05$,

respectively). D) Western blot analysis demonstrated higher PTP4A3 protein levels in colon tumors compared to normal tissue.

3.3.3 Knockout of PTP4A3 suppresses intestinal tumor formation

Wildtype and *Ptp4a3*-null mice were treated with the AOM/DSS model and tumor formation was compared by genotype. Tumors were visually obvious in the distal colon of wildtype and *Ptp4a3*-null mice upon sacrifice at both 12 and 16 weeks after the initiation of AOM/DSS treatment (Fig. 16A). Although the average number of tumors in *Ptp4a3*-null mice observed at 12 weeks was lower relative to wildtype (Fig. 16B), this was not statistically significant ($p>0.2$). However, *Ptp4a3*-null mice exhibited a 54% decrease in tumor number ($p<0.004$) following 16 weeks of treatment. The average diameter of tumors produced by this model was 3-4 mm and was not significantly different by genotype at either time point (Fig. 16C). These results indicate that knockout of PTP4A3 decreased tumor formation, but did not have an effect on tumor growth.

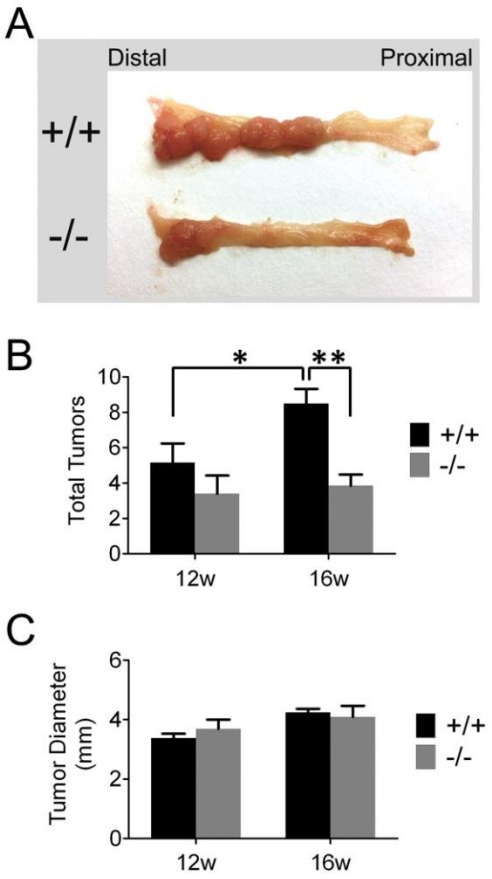

Figure 16. PTP4A3 knockout decreased colon tumor formation

A) Image depicting the appearance of wildtype and *Ptp4a3*-null colon tissue following 16 weeks treatment with AOM/DSS. B) The average number of tumors was recorded in mice by genotype after 12 and 16 weeks of treatment. The average number of tumors was significantly increased in wildtype mice between the 12 to 16 week time points ($p<0.05$). During this time the number of tumors observed in *Ptp4a3*-null mice was unchanged ($p=0.70$). At 12 weeks, wildtype mice ($n=6$) did not have significantly more tumors per mouse than *Ptp4a3*-null ($n=5$) mice ($p=0.27$). At 16 weeks, wildtype mice ($n=14$) displayed significantly fewer tumors per mouse than *Ptp4a3*-null mice ($n=7$) ($p<0.005$). C) Tumor size (measured by average tumor diameter for each mouse) was determined at each time point. No significant difference was observed in *Ptp4a3*-null mice from 12 to 16 weeks, or between genotypes at either time point.

3.3.4 Loss of PTP4A3 increases IGF1Rβ and c-MYC expression in tumors

Next, lysates obtained from both wildtype and *Ptp4a3*-null colon tumors were examined. Reverse phase protein array analysis was used to assay the levels of over 130 different protein products contained in wildtype and *Ptp4a3*-null tumors. While protein levels in these tumors exhibited considerable heterogeneity, two known oncogenic signaling proteins, the receptor tyrosine kinase IFG1Rβ and the transcription factor c-MYC, were expressed at higher levels in *Ptp4a3*-null tumors compared to wildtype controls (Fig. 17A). Following quantification of the Western blot, IGF1Rβ protein was on average 2.1-fold higher ($p<0.001$) and c-MYC was 2.5-fold higher ($p<0.02$) in *Ptp4a3*-null relative to wildtype colon tumors (Fig. 17C-D). In contrast, no significant difference in AKT activation was observed between genotypes (Fig. 17E). This result suggested that tumors could potentially compensate for PTP4A3 deficiency though altered signaling pathways.

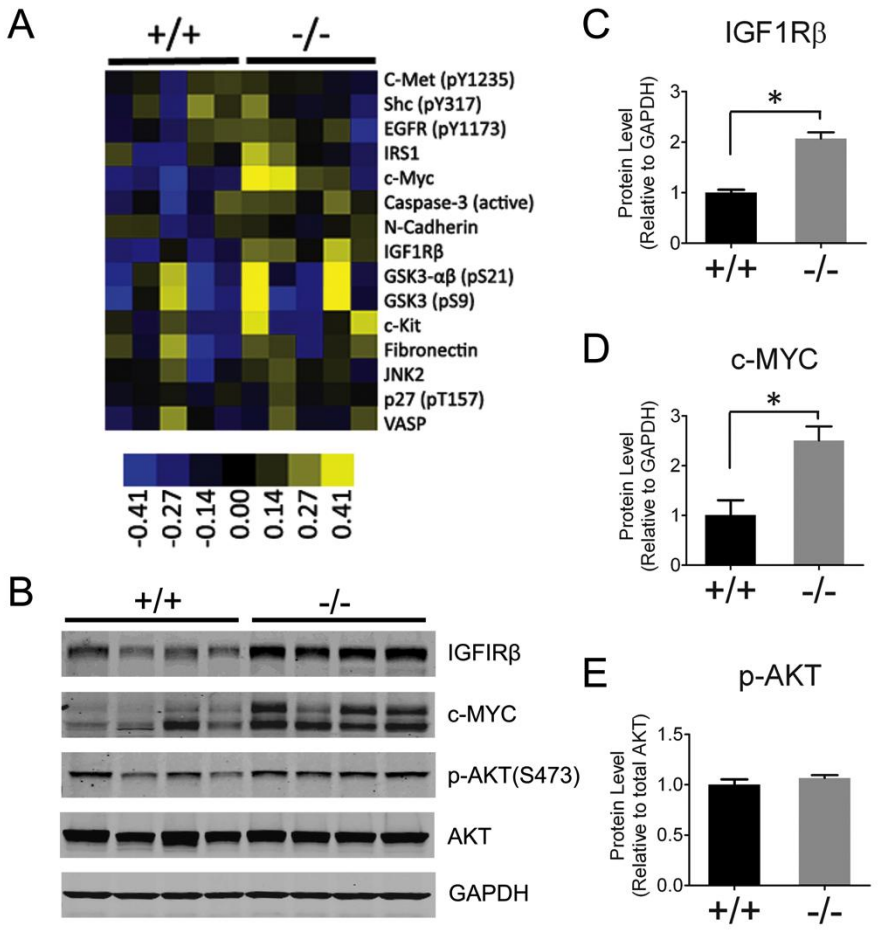

Figure 17. Higher IGF1Rβ and c-MYC protein levels were observed in *Ptp4a3*-null tumors

A) Cluster sample of the heatmap generated from RPPA analysis that was performed using colon tumor lysates from AOM-DSS treated wildtype and *Ptp4a3*-null mice. Protein targets were higher (yellow), lower (blue), or unchanged (black). B) Protein levels were confirmed by western blot analysis of colon tumor lysates from wildtype and *Ptp4a3*-null mice. IGF1Rβ and c-MYC protein were chosen because they appeared to be the most consistently upregulated proteins in *Ptp4a3*-null samples. C) When quantified, IGF1Rβ protein levels were 2.1-fold higher in *Ptp4a3*-null tumors ($p<0.001$). D) c-MYC protein levels were 2.5-fold higher in *Ptp4a3*-null tumors ($p<0.02$). E) The levels of activated AKT, as indicated by phosphorylation of Ser473, were not significantly different by genotype relative to total AKT protein.

3.3.5 c-MYC activity increases *Ptp4a3* gene expression

Because c-MYC expression appeared to be affected by *Ptp4a3* genotype, further investigation of whether there is a connection between these two genes was performed. Both c-MYC and PTP4A3 are considered to have oncogenic properties and both are overexpressed in a number of human cancers. The transcription factor c-MYC can transform cells and has the potential to regulate up to 10% of all genes. The effect of c-MYC on *Ptp4a3* gene expression was examined using transgenic MEFs expressing the chimeric Myc-Estrogen Receptor (MycER) protein. Following treatment with 4-hydroxytamofin (4-HT), MycER localizes to the nucleus where it is capable of c-MYC transcriptional regulation.

Both wildtype and MycER MEFs were untreated, treated with ethanol (vehicle control) or 4-HT for 24 hours. *Ptp4a3* gene expression was assayed by quantitative RT-PCR and wildtype MEFs exhibited similar transcript levels regardless of treatment (Fig. 18). Following 4-HT treatment, *Ptp4a3* expression in MEFs expressing MycER was elevated 3-fold relative to untreated and vehicle control treated cells. This result indicates that *Ptp4a3* gene expression is increased by c-MYC activity and PTP4A3 may be a downstream effector of oncogenic transformation by c-MYC. Upregulation of c-MYC in *Ptp4a3*-null tumors (Fig. 17D) may be a result of compensation or possibly c-MYC stabilization if PTP4A3 is able to dephosphorylate it as a form of negative feedback.

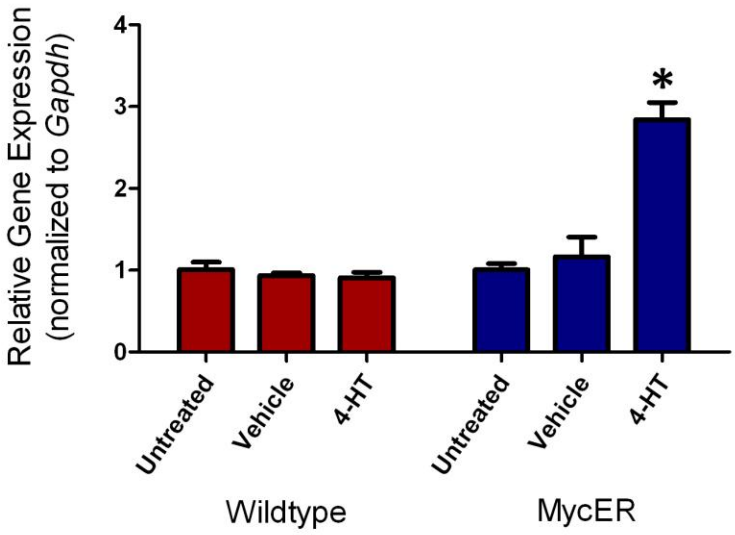

Figure 18. *Ptp4a3* gene expression was increased following c-MYC activation

Wildtype and transgenic (MycER) MEFs were control treated or treated with 4-HT. *Ptp4a3* gene expression was assayed by quantitative RT-PCR following 24 hours of treatment. A significant increase in *Ptp4a3* transcript level was observed in MycER cells following 24 hours of 4-HT treatment ($p<0.007$). No effect on gene transcription was observed in wildtype MEFs regardless of treatment.

3.4 DISCUSSION

Human PTP4A3 is strongly implicated in the pathogenesis of human metastatic colorectal cancer. Investigation of the effects of *Ptp4a3* deletion in a mouse model of colon cancer has now provided additional insight into its role in malignancy. Treatment with AOM/DSS is one of the most popular colon tumor mouse models and the C57BL/6J strain to which this model was backcrossed is particularly susceptible to colitis-associated cancer [98, 99, 102]. *Ptp4a3* is traditionally classified as a gene associated with metastasis and not known to be involved in the early stages of cancer progression. These results have demonstrated for the first time that the *Ptp4a3* message was upregulated very early following exposure to AOM (Fig. 16), the initiating

step in the colon cancer model. This is important evidence that PTP4A3 could be also involved in the pre-neoplastic stage of malignancy.

Mice subjected to the AOM/DSS model consistently developed tumors in the distal region of the colon. These primary tumors displayed consistently higher levels of *Ptp4a3* relative to normal colon epithelium (Fig. 15) - similar to what is seen in human colon cancer patients [27]. Notably, mice deficient for PTP4A3 had >50% reduction in tumor formation providing further evidence that PTP4A3 is a key mediator of colon carcinogenesis (Fig. 16). Nevertheless, the complete absence of PTP4A3 phosphatase was insufficient to abolish colon tumorigenesis, suggesting that a subset of tumors may not require PTP4A3 as a driver of the disease. The finding that not all tumors in this model had high *Ptp4a3* gene expression levels (<2-fold upregulation) further supports this conclusion.

The mouse model allowing for gene knockout presented a unique opportunity to address the role of PTP4A3 in tumor biology. AOM exposure causes DNA damage and genotoxic stress [102]. A prominent response to DNA damage is induction of p53, which can induce *Ptp4a3* gene expression [16] and may provide an explanation for the induction of *Ptp4a3* in the colon of AOM treated mice. Additionally, *Ptp4a3* has been identified as a direct regulatory target of TGFβ signaling in colon cancer cells. The active TGFβ signal induces SMAD3/4 binding to the *Ptp4a3* genomic locus and thus inhibition of gene transcription [58]. Loss of TGFβ is a frequently observed phenomenon in human colon cancer [106], as well as the AOM mouse model of colon cancer [103]. It is likely that this event contributes to elevated *Ptp4a3* gene expression in cancer through SMAD3/4 inactivation. Interestingly, a mouse model deficient for *Smad3* is reported to spontaneously develop colon cancer [107], and *Smad4* deletion greatly exacerbates a mouse model of colon cancer [108].

The formation of neoplastic lesions in the *Ptp4a3*-null mice may have been the consequence of the engagement of additional growth factor signaling pathways or oncogenes, such as IFG1Rβ and c-MYC. c-MYC is known to be increased in tumors after AOM/DSS treatment and both IFG1Rβ and c-MYC were markedly elevated in the *Ptp4a3*-null tumors relative to wildtype derived tumors (Fig. 17). Further results demonstrated that elevated c-MYC activity increased *Ptp4a3* gene expression (Fig. 18). Additional research will be required to determine if *Ptp4a3* is a direct target of c-MYC. In order to demonstrate direct interaction of c-MYC with the *Ptp4a3* gene locus, chromatin-immunoprecipitation or electromobility shift assay can be performed. The use of reporter assays in various cell types would also conclusively demonstrate transcriptional regulation of PTP4A3 by c-MYC.

While these results suggest that PTP4A3 is a mediator of carcinogenesis, it does not model the effect a PTP4A3 inhibitor would have on an existing tumor. To examine this, it would be preferable to establish colon tumors in floxed mice and subsequently knockout the *Ptp4a3* gene in the tissue. Another consideration is that a pharmacological inhibitor is likely to inhibit only the catalytic activity of PTP4A3, which may not be faithfully modeled by gene deletion. In the absence of a potent and specific PTP4A3 inhibitor for use *in vivo*, the ideal experiment would knockout functional PTP4A3 while simultaneously knocking-in the catalytically inactive PTP4A3 mutant.

4.0 PTP4A3 REGULATES VEGF SIGNALING AND PROMOTES ANGIOGENESIS

4.1 INTRODUCTION

PTP4A3 is a prenylated dual-specificity phosphatase with poorly understood enzymology and functionality [12]. Mice in which *Ptp4a3* is genetically ablated are healthy, fertile and phenotypically similar to wildtype littermates, although adult male homozygous knockout mice exhibited slightly decreased body mass [109]. Importantly, loss of PTP4A3 partially suppresses colon carcinogenesis in a mouse model of colitis associated colon cancer [109]. High levels of *Ptp4a3* gene expression, as well as its closely related family members *Ptp4a1* and *Ptp4a2*, are often associated with tumor growth and metastasis of many human cancer types [110]. Furthermore, poor patient prognosis and increased tumor invasiveness are commonly observed in malignancies expressing high levels of *Ptp4a3* [27, 49]. While the specific PTP4A3 substrates have remained elusive, several downstream signaling pathways have been proposed including: PI3K/AKT [71], SRC [65], ERK1/2 [67], and Rho GTPases [17]. Considering the multitude of proposed signaling effectors, it is likely that the function of PTP4A3 is tightly regulated by cell type and specific cues from the extracellular environment.

Clinical findings have suggested that in addition to a role in cancer cells, PTP4A3 may be fundamentally involved in angiogenesis. High *Ptp4a3* gene expression levels are observed in tumor endothelium pointing to its potential involvement in the pathological angiogenesis

mandated for tumor progression as well as metastatic colonization [111, 112]. *Ptp4a3* is increased ten-fold in the vasculature of invasive breast tumors relative to normal vasculature [113]. High PTP4A3 expression is also observed in developing heart tissue and blood vessels but not in their mature forms, suggesting a role for PTP4A3 in cardiovascular system development [26].

Angiogenesis is a multifaceted process that utilizes a complex network of growth factors and signaling pathways. Vascular Endothelial Growth Factor (VEGF) is a very well characterized pro-angiogenic factor that is able to induce proliferation, sprouting and tube formation of endothelial cells, which are necessary for the creation of new vasculature. When VEGF binds to its cognate receptors on endothelial cells, several key pathways that promote angiogenic signaling are activated. Known downstream effectors of VEGF signaling include SRC [114] and MAP kinase [115]. Interestingly, *Ptp4a3* gene expression in endothelial cells appears to be regulated by VEGF through the receptor VEGFR2 and transcription factor Myocyte Enhancer Factor 2C activity [116].

Because of the potential role of PTP4A3 in vascular function during angiogenesis, I sought to test the hypothesis that PTP4A3 is a mediator of the angiogenic phenotype of vascular cells. Accordingly, blood vessel development was contrasted in experimental colon tumors from wildtype and *Ptp4a3*-null mice using CD31 immunocytochemistry. Aspects of wound repair were quantified in primary murine pulmonary endothelial cells from wildtype and *Ptp4a3*-null mice. Furthermore, the contribution of PTP4A3 to VEGF signaling and its downstream signaling components, particularly phosphorylation of SRC was examined. This mechanism was further confirmed through pharmacologic sensitivity of SRC activation and wound repair capacity of human microvascular endothelium to a PTP4A3 inhibitor.

4.2 MATERIALS AND METHODS

4.2.1 Measurement of blood pressure and cardiovascular output

Mouse blood pressure and cardiovascular output measurements were assayed with the CODA non-invasive tail-cuff system (Kent Scientific). Adult male mice (n=5/genotype, 8-10 weeks) under normal diet and environmental conditions were used for the study. All tail cuff experiments were performed on conscious mice at approximately the same time of day (throughout 2 hours in the late morning), and body temperature was accurately controlled with a 37°C heat pad. Mice were trained on the equipment daily for 4 consecutive days before experimental data were collected. Cardiovascular statistics for each mouse were determined as the mean of at least 3 measurements taken on day 5.

4.2.2 Immunohistochemistry and microvessel density quantification

Tissues were isolated and fixed in 10% neutral buffered formalin overnight at room temperature. Tissues were then submerged in 70% ethanol and transferred to the Starzl Transplant Institute Research Histology Services core facility for processing. Briefly, samples were then embedded in paraffin and sectioned onto glass slides. Slides were then deparaffinized and antigenicity retrieved by steaming in EDTA pH 8.0 for 30 min. For the microvessel density assay, antibody against CD31 (clone M-20; Santa Cruz Biotechnology) was used at a concentration of 1:300 at room temperature overnight. For each colon cancer sample (n=4 mice/genotype), randomly chosen $CD31^{+}$ stained fields (n=5/mouse - from multiple tumors) were imaged, positively

stained vessels were counted, and genotype vessel density was determined as the average number of vessels per mm^2 of tissue.

4.2.3 Western blot analysis

Cell and tissue samples were lysed using ice cold RIPA buffer, protein concentration was quantified by Bradford assay, and all experiments were done in triplicate. Lysates were separated using Novex SDS-PAGE reagents and transferred to nitrocellulose membranes (Invitrogen). Membranes were blocked in Odyssey buffer (LI-COR Biosciences) and incubated with primary antibodies overnight followed by secondary fluorescent antibodies according to the manufacturers' instructions. Detection and signal quantification were performed with an Odyssey infrared imager (LI-COR Biosciences). The following commercially available antibodies were used: VEGFR2, p-SRC (Y416), SRC, p-ERK1/2 (T202/Y204), ERK1/2 (Cell Signaling Technology); β-tubulin (Cedarlane Laboratories).

4.2.4 Tissue explant assay

Skeletal muscle tissue biopsies (pectoral major) were isolated from mice (n=3/genotype, male, 6-8 weeks of age) and placed into warm EGM-MV (Lonza) and cut into small (≤2 mm) pieces. A collagen matrix was prepared with Type I collagen containing M199, L-glutamine, penicillin-streptomycin, sodium bicarbonate, and NaOH (Sigma Aldrich) [117]. Tissue pieces were embedded into the matrix in individual wells (n=36/mouse) of a 96-well tissue culture plate and overlaid with EGM-MV (Lonza). The assay was incubated in 5% CO_2 at 37°C for 72 hours. For

each well, the distance from the solid tissue to the furthest migrating vascular cell was measured under a bright field microscope.

4.2.5 Primary endothelial cell culture

Mouse primary endothelial cells were isolated from pulmonary tissue (n=12/genotype) as previously described [118]. Briefly, cells were cultured on a collagen matrix in 2% O_2, 5% CO_2, 93% N_2 in a hypoxic chamber using Opti-MEM (Gibco) supplemented with 10% FBS, 2 mM glutamine, 0.2% retinal derived growth factor (Vec Technologies), 10 U/ml heparin, 0.1 mM non-essential amino acid supplement (Gibco) and 55 μM β-mercaptoethanol. Commercially available human microvascular endothelial cells (HMVECs) (ScienCell) were cultured in EGM-2 (Lonza) under normoxic conditions (5% CO_2) in collagen-coated tissue culture flasks. Previously reported GFP-PTP4A3 constructs [16] were transfected using Lipofectamine 2000 (Invitrogen). The PTP4A3 inhibitor BR-1 (Santa Cruz Biotechnology) was solubilized in tissue culture grade DMSO (Sigma) and added to HMVECs at the noted concentrations in 6 or 12-well plates.

4.2.6 *In vitro* wound healing assay

Primary mouse endothelial cells and HMVECs were grown to confluence in collagen-coated 12-well tissue culture plates (BD Biosciences). Each well (n=6/genotype or treatment) was scratched longitudinally with a 200 μL pipet tip and incubated for 16 hours to allow gap closure. Cell migration distance was determined by measuring the average gap distance before and after each cell front migrated inward.

4.2.7 Phospho-tyrosine antibody array

Antibody-based arrays designed to assay differences in tyrosine phosphorylation were used according to the manufacturers protocol (Full Moon Biosciences). Whole protein lysates (60 μg) from wildtype and *Ptp4a3*-null endothelial cells were biotinylated and bound to individual antibody array slides. Secondary fluorescence was performed with Cy3-labeled streptavidin (Amersham) and slides were shipped to the manufacturer for scanning and data analysis. Relative signal intensities were determined by comparing *Ptp4a3*-null median-centered values to wildtype.

4.2.8 Reverse phase protein array

Protein lysates (100 μg) from cultured endothelial cells were denatured and shipped frozen to the University of Texas MD Anderson Cancer Center Core Facility (Houston, TX) for analysis. Briefly, we made two-fold-serial dilution of the lysates for 5 dilutions, which were then arrayed on nitrocellulose-coated slides, probed with antibodies, and visualized by diaminobenzidine colorimetric reaction. Relative protein level for each sample was determined by interpolation of each dilution curve from the standard curve antibody slide. All the data points were normalized for protein loading and transformed to linear value, which were transformed to Log_2 value and then median-centered for hierarchical cluster analysis. The heatmap was generated in Cluster 3.0 as a hierarchical cluster using Pearson Correlation and a center metric.

4.2.9 Statistics

Statistical analysis of cell and tissue based assays, as well as Western blot quantification was analyzed using the 2-tailed Student t-test. For all experiments significance was defined as $p<0.05$.

4.3 RESULTS

4.3.1 Knockout of PTP4A3 in cardiovascular tissue is not cardiotoxic

As mentioned previously, fetal heart tissue had the highest level of PTP4A3 protein when assayed by Western blot (Fig. 9). Signal quantification revealed that PTP4A3 levels were 5-fold higher in fetal heart than either adult heart or skeletal muscle (Fig. 19A). While this suggested a potential role for PTP4A3 in cardiovascular development, both adult and fetal heart tissue from *Ptp4a3*-null mice appeared histologically normal relative to wildtype (Fig. 19B). Furthermore, immunohistochemical staining for CD31 revealed the presence of a similar density of blood vessels in wildtype and *Ptp4a3*-null skeletal muscle tissue (Fig. 19B) suggesting PTP4A3 was not required for vessel development.

Cardiovascular function in adult animals was examined, since it could potentially have been affected by *Ptp4a3* deletion. Blood pressure, heart rate and tissue blood flow were measured using a non-invasive tail cuff system. Mice were acclimated to the assay system daily for 4 preliminary trials throughout the course of one week. Systolic and diastolic blood pressure and heart rate were not significantly different between genotypes when assayed on day 5 (Fig.

19C-D). Tail vein blood flow also was unaffected by the loss of PTP4A3 (Fig. 19E). Collectively, these results suggested that loss of PTP4A3 activity did not overtly affect heart or vessel development, and was not required for basal function of the cardiovascular system in adult mice under non-stressed laboratory conditions.

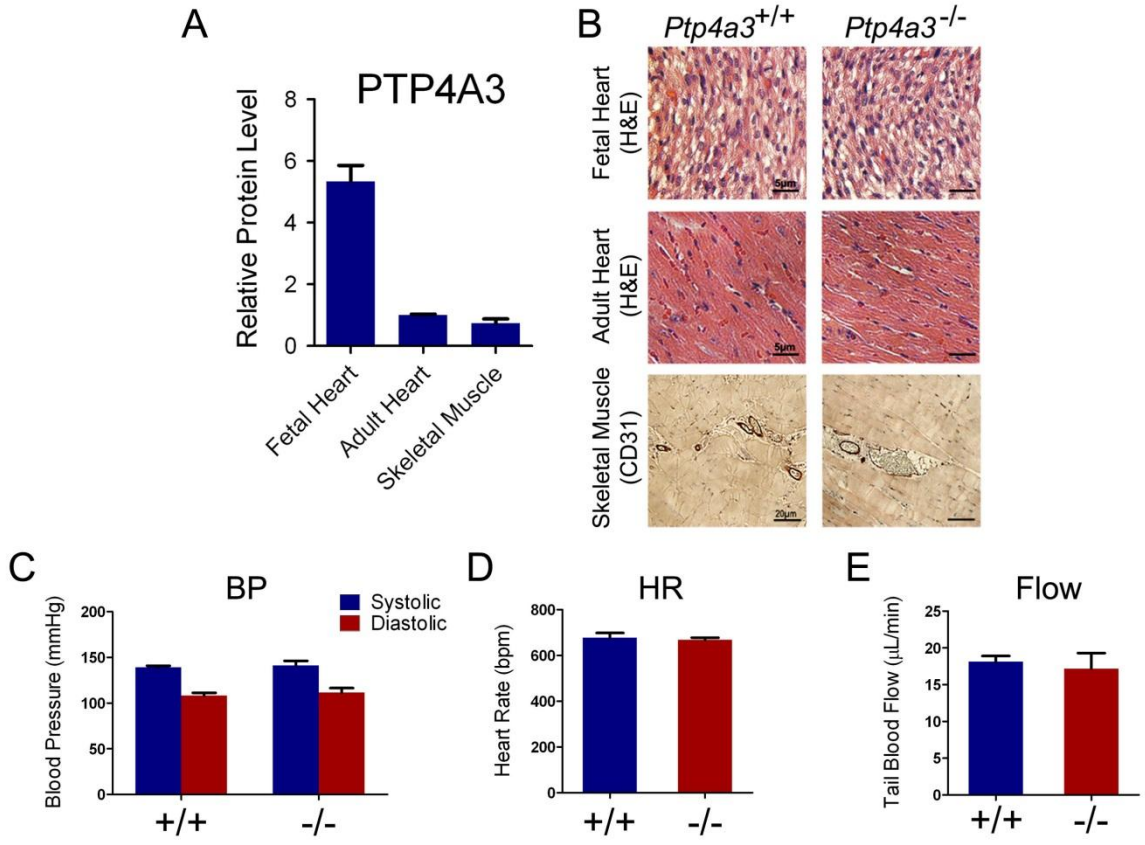

Figure 19. PTP4A3 knockout did not affect cardiovascular development or function

A) Fetal heart tissue exhibited 5-fold higher PTP4A3 protein than either adult heart or adult skeletal muscle (n=3/tissue). B) Wildtype and *Ptp4a3*-null heart tissues did not display abnormalities when examined histologically. Skeletal muscle tissue stained with antibodies against CD31 demonstrated the presence of normal vasculature. C) Blood pressure (BP) was assayed by tail-cuff and did not produce a significant difference when wildtype were compared to *Ptp4a3*-null mice (n=5/genotype). The same animals tested normally for both D) heart rate (HR), and E) blood flow through the tail vein.

4.3.2 Loss of PTP4A3 decreases tumor-driven angiogenesis

Expression of human PTP4A3 has been reported in tumor endothelium [113] and could potentially contribute to the formation of the extensive vascular network necessary for tumor growth. Colon tumor tissue from wildtype and *Ptp4a3*-null mice subject to the colitis-associated colon cancer model (AOM/DSS) [99] was examined for tumor angiogenesis. Both wildtype and knockout tumors exhibited tumor vasculature as evidenced by $CD31^+$ staining of endothelium present in both genotypes (Fig. 20A-D). Higher magnification of CD31 stained tumor tissue revealed fewer microvessels in *Ptp4a3*-null tumors compared to wildtype (Fig. 20E-H). A 30% decrease in the average microvessel density was observed in *Ptp4a3*-null tissue (Fig. 20I) revealing a critical role for PTP4A3 in the development of the tumor vascular in this mouse model of colon cancer.

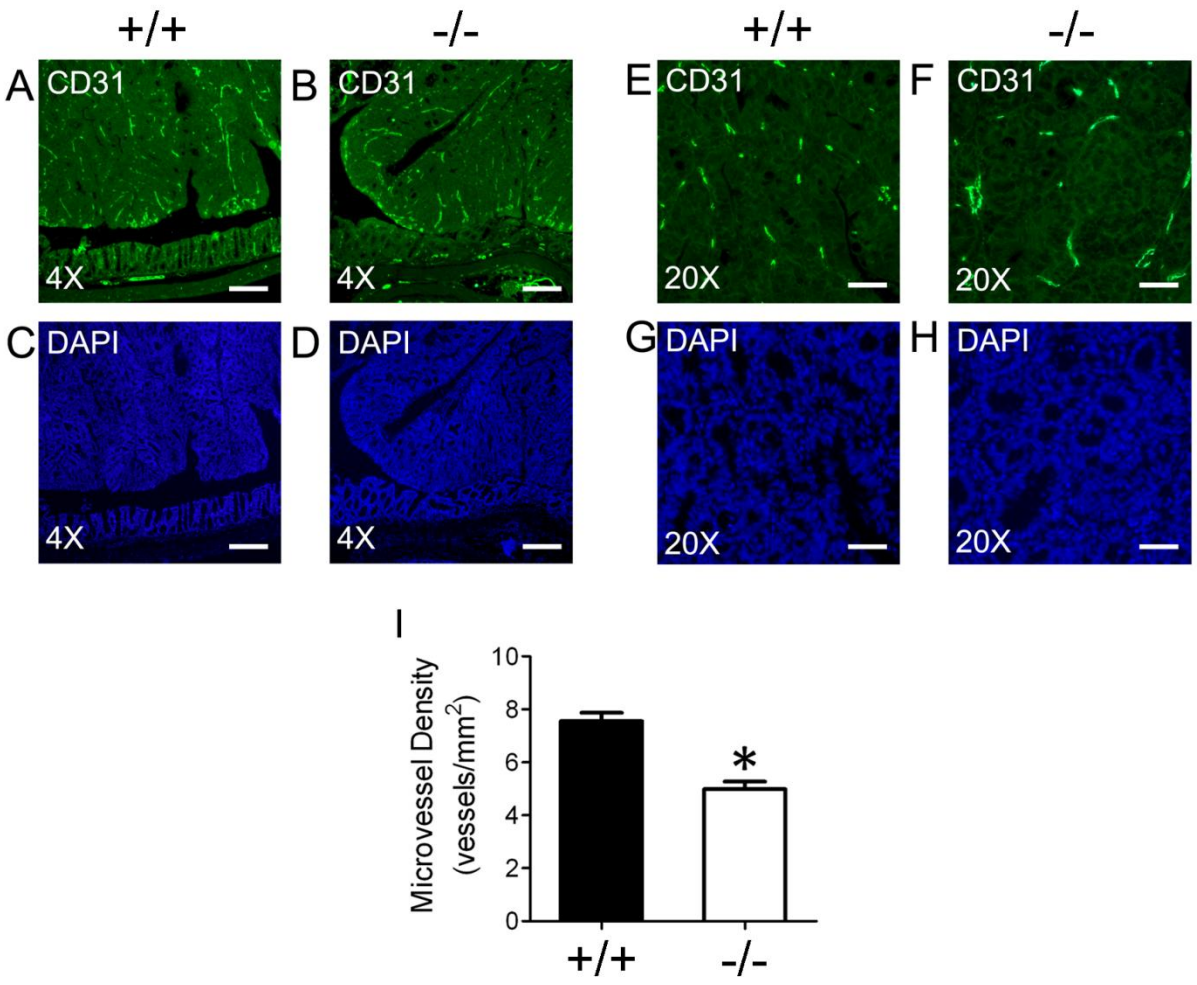

Figure 20. Decreased microvessel density in *Ptp4a3*-null colon tumors

A-B) Colon tumor and adjacent normal tissue from wildtype and *Ptp4a3*–null mice were stained for CD31 (FITC) to visualize microvessels (4X magnification). C-D) Colon tumor and adjacent normal tissue stained with DAPI (4X magnification). E-F) Wildtype and *Ptp4a3*-null tumor tissue examined under higher magnification (20X) revealed less vessel formation in knockout tissue compared to wildtype. G-H) Colon tumor and adjacent normal tissue stained with DAPI (20X magnification). I) *Ptp4a3*-null tumor tissue demonstrated a 30% reduction in $CD31^+$ microvessel density ($p<0.001$).

4.3.3 Loss of PTP4A3 decreases vascular cell invasion

Angiogenic phenotype was then examined in tissues with and without functional PTP4A3. An *ex vivo* invasion assay that models wound healing was implemented using skeletal muscle tissue biopsies that were capable of producing outgrowth of vascular cells in response to external stimuli [117]. Tissue samples were embedded in a Type I collagen matrix containing microvascular endothelial growth medium (Fig. 21A-B). The resulting outgrowth of cells into the matrix has been commonly used as a measure of angiogenesis [117]. When examined under higher magnification, the apical nature of invasive endothelial cells in the three dimensional matrix became apparent (Fig. 21C). Compared to wildtype tissue, the *Ptp4a3*-null samples resulted in reduced outgrowth as measured by the distance from the solid tissue to the furthest invading cell. The average invasion distance after incubation for 72 hours was 20% less in *Ptp4a3*–null cells compared to wildtype cells (Fig. 21D). This result suggested PTP4A3 was a contributing factor to the invasive potential of vascular cells.

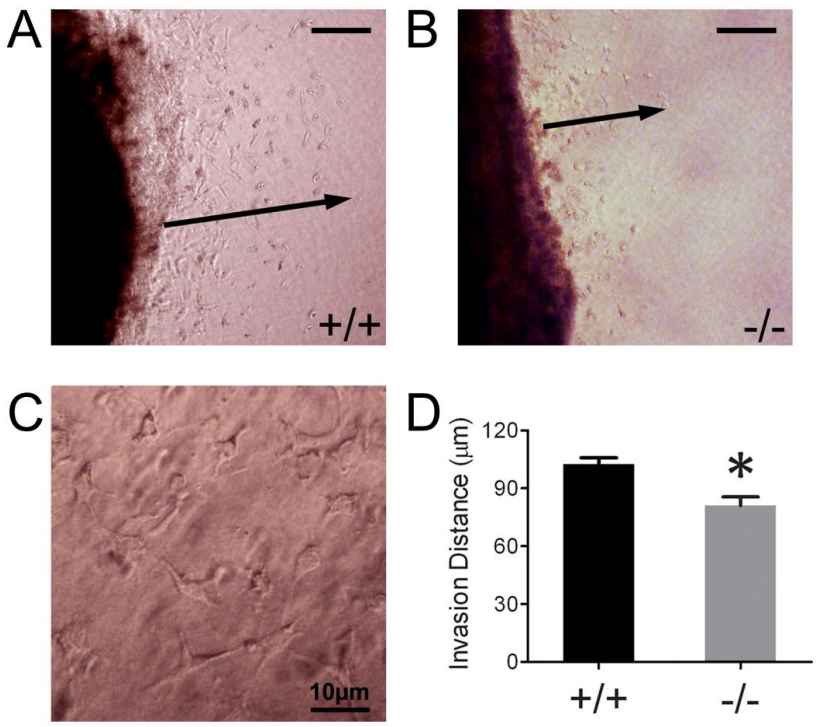

Figure 21. PTP4A3 knockout tissue exhibited reduced vascular cell invasion *ex vivo*

Skeletal muscle tissue biopsies from wildtype (A) and *Ptp4a3*-null (B) mice were embedded in a 3-dimensional collagen matrix allowing for outgrowth of vascular cells. The distance of the furthest migrating cell (arrow) was measured for each tissue explant (bar=50µm). C) Endothelial cells examined under higher magnification displayed an apical appearance when invading the matrix (bar=10µm). D) Cells from *Ptp4a3*-null tissue exhibited a 20% decrease in invasion distance compared to cells expressing PTP4A3 (*$p<0.02$).

4.3.4 PTP4A3 knockout endothelial cells exhibit reduced cell migration

Primary pulmonary endothelial cells from adult wildtype and *Ptp4a3*-null mice were isolated and cultured *in vitro*. Cell migration potential was assayed using an *in vitro* wound healing assay [119] in which endothelial cells were grown to confluence and a longitudinal gap was created. These cells were incubated for 16 hours to permit gap closure via endothelial migration (Fig. 22A-D). Following incubation for 16 hours, cell migration distance was measured in both

genotypes. On average *Ptp4a3*-null cells migrated 50% less than the corresponding wildtype cells (Fig. 22E). These results suggested a functional role for PTP4A3 in endothelial migration, another process required for angiogenesis.

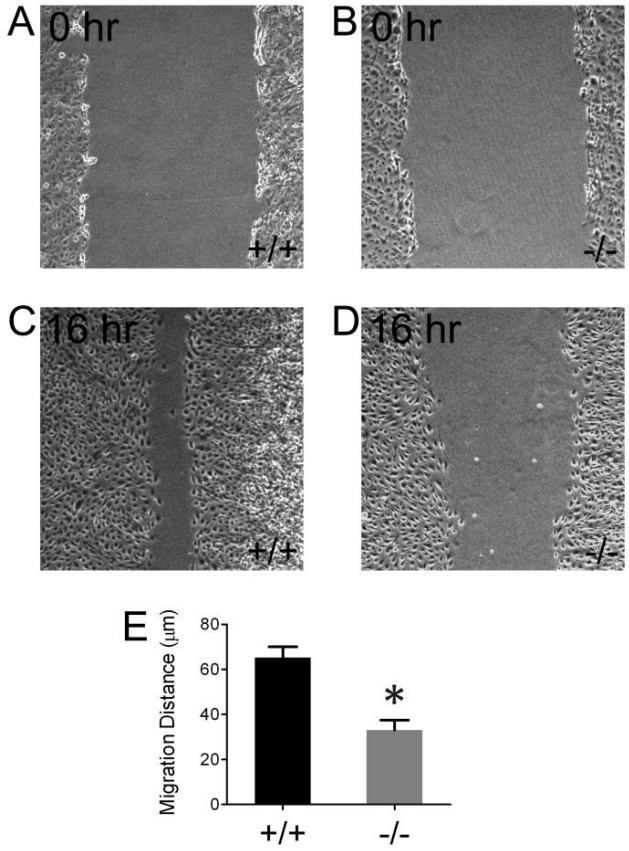

Figure 22. Knockout of PTP4A3 in endothelial cells decreased migration *in vitro*

A-D) Pulmonary endothelial cells were purified from wildtype and *Ptp4a3*-null mice, seeded evenly and grown to confluence in collagenized cell culture plates. Cells were then scratched with a pipet tip and allowed to migrate for 16 hours. E) Migration distance was measured following gap closure. *Ptp4a3*-null cells migrated 50% less compared to wildtype endothelial cells (*$p<0.001$).

4.3.5 Loss of PTP4A3 alters angiogenic signaling pathways

It has been recently reported that *Ptp4a3* gene expression is induced in endothelial cells following VEGF treatment [116] but the distal effects of PTP4A3 in the endothelium have not

yet been explored. Disruptions in cellular signaling pathways were examined as a mechanistic basis for the reduced migration and invasion in *Ptp4a3*-null endothelial cells.

First, protein lysates from cultured endothelium were examined with phospho-tyrosine antibody arrays (Fig. 23). Most of the targets identified as being altered by genotype had not previously been implicated in the function of PTP4A3, and further analysis will be required to determine their relevance in this system. However, several proteins involved in cell migration including SRC and FAK were identified as differentially phosphorylated in *Ptp4a3*-null cells indicating a possible impairment in focal adhesion turnover (Fig. 23A). Additionally, several receptor tyrosine kinases including VEGFR2, PDGFRβ and FGFR1 were less phosphorylated at certain tyrosine residues even though these cells were cultured under the same conditions and in the presence of the same growth factors (Fig. 23B).

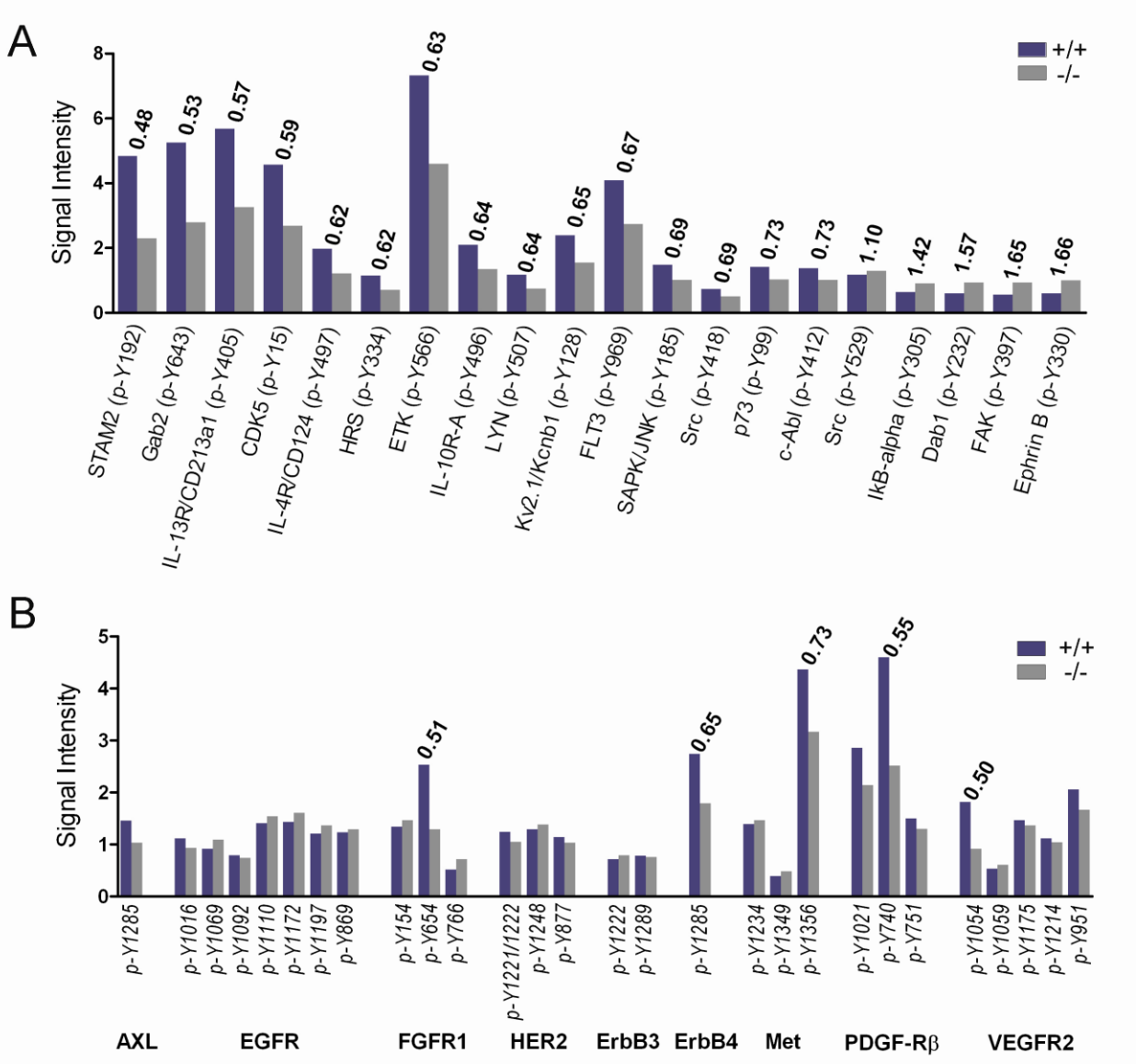

Figure 23. Altered tyrosine phosphorylation in wildtype and *Ptp4a3*-null endothelial cells

Cultured endothelial cells were assayed for protein tyrosine phosphorylation by antibody array. A) Multiple tyrosine residues on various protein targets exhibited different levels of phosphorylation in wildtype compared to *Ptp4a3*-null cells. B) Tyrosine residues of various receptor proteins exhibited differential phosphorylation profiles in wildtype and *Ptp4a3*-null cells. Numbers indicate the relative signal strength of *Ptp4a3*-null relative to wildtype sample.

Endothelial cells from wildtype and *Ptp4a3*-null pulmonary tissue were cultured and incubated in serum-free medium and treated with recombinant VEGF for up to 8 hours. Two

known VEGF-dependent mediators of the angiogenic phenotype, SRC and ERK1/2, have also been associated with PTP4A3 signaling [65, 67]. Activation of both proteins from wildtype and *Ptp4a3*-null endothelial cells was determined by assaying their phosphorylation status with Western blotting (Fig. 24A). A significant increase in SRC protein phosphorylation (Y416) was observed in wildtype cells within 15 min following VEGF treatment, and persisted up to 8 hours (Fig. 26B). Comparatively, *Ptp4a3*-null endothelial cells did not exhibit an increase in SRC phosphorylation at any time point following VEGF exposure. An increase in ERK1/2 phosphorylation was observed in both genotypes following treatment with VEGF (Fig. 24A). Levels of total SRC and ERK1/2 protein were unchanged throughout this time course. As expected, mature VEGFR2 protein levels decreased in both genotypes following VEGF treatment, presumably due to internalization of the receptor upon activation. This finding indicated that PTP4A3 was essential for VEGF-induced activation of SRC, but not necessary for ERK1/2 activation in endothelial cells. The mechanism for control of SRC activation by PTP4A3 is not obvious and this data does indicate a direct substrate interaction. Therefore, it is likely that PTP4A3 has a substrate that is upstream in the cascade that activates SRC.

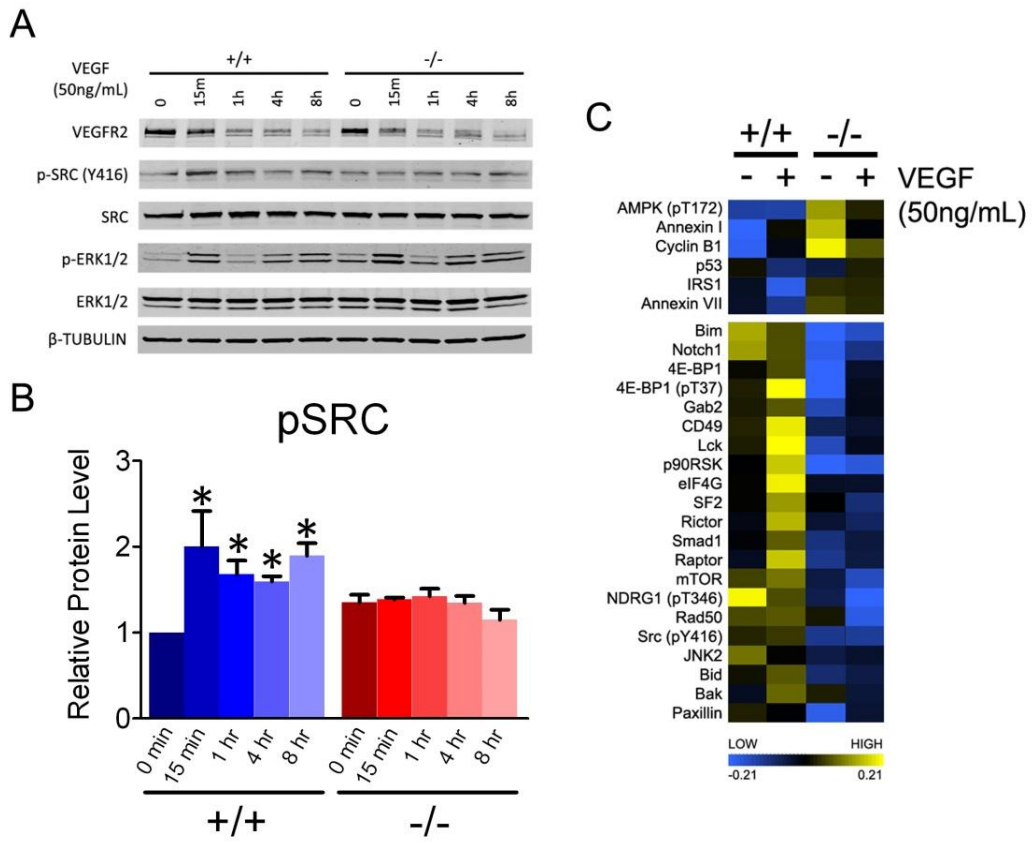

Figure 24. PTP4A3 participated in the endothelial cellular response to VEGF exposure

A) Wildtype and *Ptp4a3*-null endothelial cells were grown in culture and treated with VEGF (50 ng/mL) for up to 8 hours. Protein lysates were collected at various time points and Western blot was performed to assay the levels of known mediators of the angiogenic processes, including SRC and ERK1/2. B) In wildtype cells, phospho-SRC (activated) was increased nearly 2-fold following 15 min of VEGF treatment, and phosphorylation was significantly increased up to 8 hours later. Increased activation of SRC was not observed at any time point when *Ptp4a3*-null cells were treated with VEGF. C) Reverse phase protein analysis was performed on lysates from wildtype and *Ptp4a3*-null endothelial cells treated with either VEGF (50 ng/mL) or vehicle control (saline). The depicted heatmap shows a subset of protein targets that were differentially altered by VEGF treatment.

RPPA analysis was performed to determine the levels of 130 different phosphorylated and non-phosphorylated proteins from lysates obtained from wildtype and *Ptp4a3*-null endothelial cells. Cultured endothelial cells were treated for 8 hours with serum-free medium

containing either PBS (control) or VEGF (50 ng/mL). Summarized in Fig. 24C are protein level differences that appeared altered by genotype, which suggested that PTP4A3 mediates the effect of VEGF on several key signaling pathways. It is noteworthy that SRC phosphorylation (pY416) was increased in VEGF-treated wildtype cells while it was unaffected in *Ptp4a3*-null cells. Additionally, several other proteins were either increased in abundance or hyperphosphorylated upon VEGF treatment in wildtype endothelial cells but not *Ptp4a3*-null cells including: p90RSK, eIF4G, SF2, and Rictor (Fig. 24C).

Interestingly, p53 protein, which was reported to be a *Ptp4a3* expression regulator [16], appeared decreased in the wildtype cells following VEGF treatment and slightly increased following VEGF treatment in *Ptp4a3*-null endothelial cells. This could be the result of a negative feedback mechanism in which PTP4A3 regulates p53 levels [57].

4.3.6 Pharmacological inhibition of PTP4A3 impaired HMVEC migration

The cellular localization of PTP4A3 protein is likely important for its function and facilitation of migration in endothelial cells. When ectopically overexpressed in HMVECs, a GFP-PTP4A3 construct displayed a distinct cellular localization pattern compared to the diffuse cytoplasmic fluorescence of GFP alone as seen 24 hours after transfection (Fig. 25A). The GFP-PTP4A3 protein was typically associated with the plasma membrane and/or endosomal compartment, which is consistent with previously reported results in other cell types [14]. Additionally, *Ptp4a3* overexpression appeared to result in lamellipodia formation in these cells that is necessary for cellular migration and invasion (Fig. 25A). This was also accompanied by a change in cell shape as GFP cells exhibited a rounder appearance while GFP-PTP4A3 cells were more apical.

The effect of BR-1 on motility and signal transduction of HMVECs was then assessed. BR-1 was chosen as opposed to other PTP4A3 inhibitors because it is relatively potent, considered to be specific for PTP4A3, and commercially available. Native HMVECs were treated with BR-1 and displayed a concentration dependent decrease in endothelial cell motility when examined in a wound healing assay (Fig. 25B-C). Lysates were obtained from BR-1 treated HMVECs cultured in the presence of growth factors, and assayed for SRC protein by Western blot (Fig. 25D). The level of SRC phosphorylation (Y416) was significantly decreased relative to total SRC protein that was unchanged (Fig. 25E). This indicated that BR-1 treatment suppressed the SRC pathway and supported a mechanism by which PTP4A3 mediates VEGF-induced endothelial cell motility by activating SRC signaling.

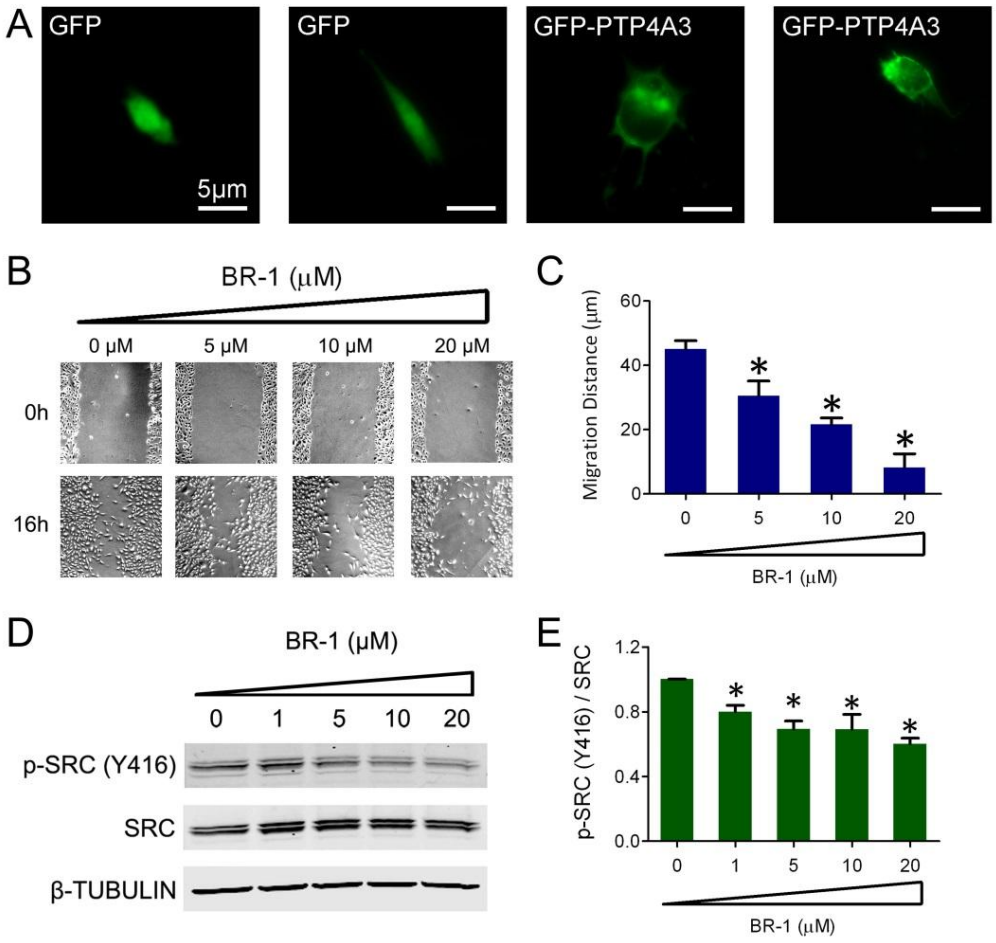

Figure 25. PTP4A3 inhibition reduced HMVEC migration and SRC activation

A) HMVECs transfected with GFP or GFP-PTP4A3 were cultured for 24 hours and imaged using fluorescence microscopy. B-C) HMVECs exhibit a significant decrease in migration when treated with 5-20 μM BR-1 (*$p<0.02$). D) Lysates from HMVECs treated with the PTP4A3 inhibitor BR-1 were collected and assayed by Western blot for SRC phosphorylation (Y416). E) Quantification of p-SRC relative to total SRC revealed a decrease in active SRC following PTP4A3 inhibition (0μM>1μM *$p<0.01$) which was also determined to be concentration dependent (1μM>20μM *$p<0.02$). Representative images of HMVECs treated with BR-1 or a DMSO vehicle control and incubated for 16 hours.

4.4 DISCUSSION

Although the precise function of PTP4A3 remains unclear, it is closely associated with cancer progression and metastasis [112]. Elevated *Ptp4a3* gene expression, especially in colorectal tumors, is a useful biomarker and represent a potential novel therapeutic target [27]. It is becoming clear that PTP4A3 can functionally contribute to multiple aspects of neoplasia including tumor formation, metastasis, and angiogenesis. Importantly, *Ptp4a3* expression has been reported to be regulated by p53 [16], TGFβ [58], and VEGF [116], all of which have been implicated in endothelial cell function during angiogenesis.

Ptp4a3-null mice were phenotypically similar to their wildtype littermates under standard conditions in terms of cardiac and skeletal muscle morphometry and vascularity, blood pressure, heart rate and peripheral (e.g. tail vein) blood flow (Fig. 19). Nonetheless, the gene deletion model revealed that colon tumors deficient for PTP4A3 had reduced microvessel density when compared to wildtype tumors (Fig. 20). Additionally, endothelial cells lacking PTP4A3 were less invasive and migratory when assayed *ex vivo* (Fig. 21-22). The tissue explant assay models an important early step in the angiogenic process when cells invade the basal lamina as a precursor to vessel sprouting. Tissue samples from *Ptp4a3*–null mice displayed significantly less invasive capacity measured by this assay (Fig. 21). Likewise, the *in vitro* wound healing assay demonstrates that when PTP4A3 was knocked out or pharmacologically inhibited endothelial cells were significantly deficient in gap closure (Fig. 22). Because of the length of this assay (16 hours) and the required doubling time of primary endothelial cells (>30 hours) this effect was likely due to an impairment of cellular migration, although an effect on cell proliferation cannot be excluded. A specific effect on endothelial migration could be demonstrated by either

mitotically inactivating the cells prior to the assay, or conclusively eliminating a proliferation phenotype in the knockout cells.

The results presented here suggested that several signaling proteins (particularly SRC) were affected by the absence of PTP4A3 in this cell system. We performed protein array profiling on wildtype and *Ptp4a3*-null endothelial cells in the absence or presence of VEGF in the culture medium (Fig. 24). PTP4A3 overexpression has been previously associated with increased migration and invasion in cancer cell lines [120] and could conceivably have a role in these processes in nonmalignant stromal cell types such as endothelial. The current results supported this hypothesis and suggest SRC could be a downstream effector of PTP4A3 in endothelial cells, as *Ptp4a3*-null cells completely lost the ability to increase SRC activation following VEGF exposure (Fig. 24). The absence of a phenotype in normal mice suggests that PTP4A3 may have a specific contribution to the process of pathological angiogenesis, which is a unique process compared to vasculogenesis.

Additionally, protein profiling identified several other signaling pathways that were altered by *Ptp4a3* genotype including various p53 and mTOR associated genes. Interestingly, p53 has been previously reported to regulate *Ptp4a3* transcription in embryonic fibroblasts [16]. It has been previously reported that p53 has a role in the angiogenic phenotype of endothelial cells [121], thus regulation by PTP4A3 could be significant in this context. There is also information suggesting PTP4A3 may have a role in mTOR signaling as the mTOR-associated protein FKBP38 has been suggested to regulate PTP4A3 protein stability [122]. Similar to p53, the mTOR pathway is also thought to function in endothelial cell signaling during angiogenesis [123].

Human microvascular endothelial cells were examined following treatment with increasing concentrations of the PTP4A3 inhibitor BR-1, and observed a concentration-dependent decrease in SRC activation evidenced by less phosphorylation at Tyr416 (Fig. 27). This effect was likely to result in an impairment of focal adhesion turnover, which supports the observed decrease in cell migration following BR-1 treatment. This could be further examined by examining focal adhesion complex formation and disassembly in wildtype and *Ptp4a3*-null cells.

Because PTP4A3 is expressed in the heart and developing cardiovascular system, there has been concern over the safety and potential cardiotoxic side effects of PTP4A3 inhibitors. These results demonstrate that mice without functional PTP4A3 are able to develop normally and do not have an overt cardiovascular phenotype under standard conditions. Moreover, *Ptp4a3*-null mice did not exhibit altered blood pressure or heart rate suggesting that the function of the cardiovascular system was not adversely affected by PTP4A3 loss. Given this information, it does not appear likely that PTP4A3 inhibition in animals would have off target effects on the cardiovascular system.

PTP4A3 has considerable potential as target for the treatment of multiple forms of malignancy due to high expression levels observed in human tumors and frequent associations with cancer cell invasiveness. Interestingly, PTP4A3 is also expressed in the tumor vasculature and may be an important mediator of pathological angiogenesis, which is an essential process for tumor progression and metastasis. Therefore, it is conceivable that attempts to therapeutically target PTP4A3 in cancer cells may also have the added benefit of inhibiting tumor angiogenesis by inhibiting PTP4A3 in the vasculature. The results presented here support this hypothesis by demonstrating that *Ptp4a3*-deficient cells and tissues have a reduced angiogenic phenotype.

Targeting the VEGF signaling pathway is a proven and clinically effective means of treating multiple human cancers including primary and metastatic tumors of the colon [124], lung [125], and kidney [126]. Unfortunately, some tumors are intrinsically resistant to or become resistant to treatments targeting the VEGF receptor as is commonly seen with antibody-based therapeutics [127]. For this reason, downstream VEGF targets are actively sought as multiple opportunities exist for therapeutic intervention.

The specific mechanism by which VEGF induces SRC activity is not completely known. Inability of the knockout cells to phosphorylate the Tyr-416 residue of SRC does not suggest that this is a direct PTP4A3 target since this observation would indicate the loss of kinase activity. One possibility is that PTP4A3 directly controls the activity of a kinase that is able to phosphorylate SRC protein. Regardless of what the direct substrate is, this data suggests that PTP4A3 is functioning upstream of SRC in endothelial cells. The cellular response to VEGF exposure is complex and diverse, so it is not surprising that loss of PTP4A3 could have an effect on some pathways and not others. A more comprehensive analysis of the proteins affected by PTP4A3 loss in these cells, specifically those associated with the SRC pathway, my shed light of the specific role of PTP4A3 in this system.

These results add novel *in vivo* evidence that PTP4A3 has a vital role in controlling the migratory and invasive properties of nonmalignant cells, specifically endothelial cells. PTP4A3 appears to be an attractive therapeutic target downstream of the VEGF signaling cascade and could theoretically be involved in many conditions involving pathological angiogenesis including cancer, diabetes, macular degeneration and cardiovascular dysfunction.

5.0 FINAL DISCUSSION

5.1.1 Conclusions and significance

The results presented in this thesis are the first to definitively examine the role of PTP4A3 in an animal model. While PTP4A3 has been studied extensively in cultured human cancer cells, little is known about its function in the *in vivo* processes that contribute to cancer. The overall goal of this project was to determine if loss of the PTP4A3 gene affected both normal mouse development and the pathology of cancer in animals. While standard tissue culture and *in vitro* techniques have been indispensable in achieving our current understanding of the processes that drive malignancy, *in vivo* carcinogenesis cannot be faithfully recapitulated outside of model organisms. Therefore, a significant disconnect exists between clinical associations with malignancy and how PTP4A3 has been proposed to function in cells. The only way to establish a concrete role for PTP4A3 in the *in vivo* malignant phenotype of cancer was to examine its function in animals.

Mice that are completely deficient for PTP4A3 expression did not exhibit a strong phenotype under normal conditions. Physiologically and metabolically they were not significantly different from littermates that express normal PTP4A3, which indicated PTP4A3 does not have an essential role in the biology of developing and adult mice. The only difference observed under normal conditions was that male homozygous knockout mice exhibited a slight

decrease in body mass and fewer homozygous knockout males were observed than was expected by standard genetics. The etiology of both these phenotypes is not immediately clear but worthy of further investigation. It is possible that PTP4A1 and PTP4A2 may be able to facilitate some of the functions of PTP4A3. Despite a normal histological profile, decreased body mass (Fig. 10) suggested a potential role in cell proliferation. Further research will be required to determine if there is a concrete basis for this phenotype or if this is an artifact of gene deletion.

The creation of a knockout mouse model afforded the unique opportunity to examine the potential for a functional contribution of PTP4A3 to *in vivo* carcinogenesis – a facet not previously studied. The hypothesis that PTP4A3 gene activity facilitates *in vivo* cellular proliferation and invasion necessary for malignant phenotype was tested. While the PTP4A3 gene product initially was thought to only be involved in tumor metastasis and late stage disease, expression in non-malignant cells and tissues provided strong evidence for possible roles at other stages of the disease. Surprisingly, *Ptp4a3* gene expression was elevated in the colon immediately following treatment with AOM (Fig. 14). The cause of *Ptp4a3* upregulation in this tissue is not immediately clear, although it could be related to p53 activation in response to genotoxic stress cause by the carcinogen. Another potential mechanism for the expression of *Ptp4a3* during oncogenic transformation could be through activation by c-MYC. The data presented here clearly indicated that *Ptp4a3* gene expression was increased as the result of c-MYC activity and could very well be an important factor in tumorigenesis. The observation that mice deficient for PTP4A3 were able to suppress colon carcinogenesis (Fig. 16) supports this conclusion and suggests that PTP4A3 maybe be an effective therapeutic target at multiple stages of cancer as opposed to only the metastatic cascade.

Primary colon tumors isolated from mice exhibited elevated *Ptp4a3* mRNA and protein (Fig. 15), a finding that was also observed in human colon tumors [27]. Interestingly, a considerable amount of variability in *Ptp4a3* gene expression was observed when comparing individual tumor samples. A subset of tumors expressed relatively low *Ptp4a3* expression levels that were similar to the adjacent normal tissue. This could potentially explain why only a partial inhibition of tumor formation was observed in *Ptp4a3*-null mice. Because similar variability in *Ptp4a3* gene expression was observed in human tumor samples [27], this could have treatment implications because it would suggests that tumors not expressing PTP4A3 may not be directly affected by PTP4A3 -targeted therapy.

The role of PTP4A3 in the process of angiogenesis is another mechanism by which it is thought to contribute to malignancy. The concept of therapeutically targeting PTP4A3 in cancer could therefore have benefits in multiple facets of the disease (i.e. simultaneously targeting cancer cells and the tumor endothelium). The results presented here clearly suggest that *Ptp4a3*-null mice had a reduced angiogenic response and that PTP4A3 likely contributed to the molecular response to VEGF exposure in endothelial cells. AOM-derived colon tumors exhibited less microvessel density in *Ptp4a3*-null mice relative to wildtype tumors (Fig. 20). Additionally, endothelial cells derived from *Ptp4a3*-null mice showed less migration and invasion when assayed *in vitro* (Fig. 21-22). This may be explained by the inability of endothelial cells to activate SRC protein in response to VEGF signals (Fig. 24).

The obvious implication of these results is that inhibiting PTP4A3 activity could reduce tumor angiogenesis and thus suppress cancer progression. The additional consequence is that PTP4A3 could also be a valuable target for the many other disease states that require pathological angiogenesis such as: diabetes, macular degeneration and cardiovascular

dysfunction. Much more investigation regarding the function of PTP4A3 in endothelium is likely required before its therapeutic value in preventing angiogenesis can be established. The newly created animal model presented here should be very useful in facilitating this work.

Based on the *in vivo* data presented in this thesis it seems unlikely that inhibition of PTP4A3 in the vasculature will be sufficient to treat cancer - although reduced, tumor angiogenesis still occurred in *Ptp4a3*-null mice. Combination therapy with VEGF antagonists or other anti-angiogenic therapies are likely worth exploring since loss of PTP4A3 only appeared to mitigate some of the response of endothelial cells to VEGF (i.e., SRC activation was prevented but ERK1/2 activation occurred). It could also be possible that the family members PTP4A1 and PTP4A2 were able to partially compensate for loss of PTP4A3 in these cells. If that is the case then a pan-PTP4A inhibitor may have significant therapeutic benefit.

In conclusion, PTP4A3 gene activity likely facilitates the *in vivo* cellular properties necessary for a malignant phenotype. Establishing that deletion of *Ptp4a3* has a necessary function in a mouse model of colon cancer suggests strong therapeutic implications throughout the progression of the disease. Although additional questions remain regarding its mechanism, this is an important milestone in understanding the biological role of PTP4A3.

5.1.2 Future directions

The results presented here strongly suggest a role for PTP4A3 in both carcinogenesis and angiogenesis. Experiments in both aims of this thesis have provided mechanistic insight regarding the function of PTP4A3, although a clear, unified mechanism of action is still at large. The single greatest obstacle in our understanding of the true biological role of PTP4A3 is the lack of a direct known substrate. Several proteins were identified as having higher tyrosine

phosphorylation in *Ptp4a3*-null endothelial cells: EphrinB (pTyr-330), FAK (pTyr-397), Dab1 (pTyr-232) and IkB-α (pTyr-305). Higher phosphorylation would be expected for the substrate of a phosphatase that was deleted in the cell, and these targets should be further investigated for their potential as direct phospho-substrates.

The knockout mouse model provides an extremely valuable tool for studying the function of PTP4A3 both phenotypically and mechanistically. Many mouse models of cancer have been developed in recent years and it would be very interesting to examine the effect of *Ptp4a3* knockout in different cancer types such as liver, breast, or leukemia. In addition to cancer, mouse models of many human diseases including obesity, diabetes, hypertension and stroke are frequently used in biomedical research and could provide insight about a potential role for PTP4A3 in these conditions.

One of the greatest strengths of this targeted animal model is the ability to perform temporal or tissue specific knockout of PTP4A3. Global deletion was chosen for this study because knockout of PTP4A3 had not been previously reported and the potential for an effect on multiple systems existed. The limitation of this approach is that when studying a complex phenomenon that involves multiples cell types (such as cancer) the effect of knockout could be relevant to a specific system that cannot be easily distinguished from the observations. For example, suppression of colon cancer in *Ptp4a3*-null mice could be the result of gene deletion in the colon epithelium, peripheral vasculature, stroma, immune cells or all of these systems combined. Testing the cancer model following conditional knockout of PTP4A3 in individual systems would demonstrate the importance of PTP4A3 function in that cell type and would likely provide considerable insight about the role of PTP4A3 in cancer. For example, the *Ptp4a3* floxed allele could be crossed to transgenic mice expressing Cre recombinase from the *Vil1*

promoter to facilitate PTP4A3 knockout specifically in intestinal epithelial cells [128]. When challenged with AOM/DSS, a significant difference in colon carcinogenesis in these mice would be attributable to the function of PTP4A3 in colon tumor (or pre-neoplastic colon) cells.

Additionally, since the PTP4A genes are likely to have similar and potentially overlapping functional roles, multiple *Ptp4a* isoform knockout mice would be very interesting to examine. A knockout mouse model for PTP4A2 has recently been reported [24] and it is likely that a PTP4A1 knockout model will be available in the future. Crossing these strains to create multiple null mutations could add considerable insight about the *in vivo* function of this gene family.

Finally, gene deletion is an important technique for studying the role of therapeutic targets in animals. However, the action of a potent yet reversible phosphatase inhibitor would likely have a somewhat different effect on a biological system than the null mutation. The effort to understand and evaluate the value of PTP4A3 as an anti-cancer target would be greatly aided by the availability of additional effective and specific small molecule inhibitors. Several compounds that inhibit PTP4A3 have been identified but none have been characterized in vivo. A comprehensive pharmacological toolbox will ultimately be required to exploit PTP4A3 for treatment of human malignancy.

APPENDIX A

FREQUENTLY USED ABBREVIATIONS

Abbreviation	Full terminology
AML	Acute Myelogenous Leukemia
AOM	Azoxymethane
BMI	Body Mass Index
BR-1	Benzylidine Rhodanine 1
BrdU	Bromodeoxyuridine
BUN	Blood Urea Nitrogen
CML	Chronic Myelogenous Leukemia
CSK	C-Terminal SRC Kinase
DSP	Dual Specificity Phosphatase
DSS	Dextran Sodium Sulfate
eIF2	Elongation Initiation Factor 2
EMT	Epithelial To Mesenchymal Transition
ES	Embryonic Stem
GFP	Green Fluorescent Protein
HMVEC	Human Microvascular Endothelial Cell
IGF1Rβ	Insulin-Like Growth Factor Receptor 1β
NEO	Neomycin Resistance Cassette
PRL	Phosphatase of Regenerating Liver
PTP	Protein Tyrosine Phosphatase
ROCK	Rho Kinase
TGFβ	Transforming Growth Factor B

BIBLIOGRAPHY

1. Hunter, T., *Why nature chose phosphate to modify proteins.* Philos Trans R Soc Lond B Biol Sci, 2012. **367**(1602): p. 2513-6.

2. Alonso, A., et al., *Protein tyrosine phosphatases in the human genome.* Cell, 2004. **117**(6): p. 699-711.

3. Hendriks, W.J., et al., *Protein tyrosine phosphatases: functional inferences from mouse models and human diseases.* FEBS J, 2008. **275**(5): p. 816-30.

4. Julien, S.G., et al., *Inside the human cancer tyrosine phosphatome.* Nat Rev Cancer, 2011. **11**(1): p. 35-49.

5. Wang, Z., et al., *Mutational analysis of the tyrosine phosphatome in colorectal cancers.* Science, 2004. **304**(5674): p. 1164-6.

6. Julien, S.G., et al., *Protein tyrosine phosphatase 1B deficiency or inhibition delays ErbB2-induced mammary tumorigenesis and protects from lung metastasis.* Nat Genet, 2007. **39**(3): p. 338-46.

7. Nagata, A., et al., *An additional homolog of the fission yeast cdc25+ gene occurs in humans and is highly expressed in some cancer cells.* New Biol, 1991. **3**(10): p. 959-68.

8. Saha, S., et al., *A phosphatase associated with metastasis of colorectal cancer.* Science, 2001. **294**(5545): p. 1343-6.

9. Zhang, J., P.L. Yang, and N.S. Gray, *Targeting cancer with small molecule kinase inhibitors.* Nat Rev Cancer, 2009. **9**(1): p. 28-39.

10. Mohn, K.L., et al., *The immediate-early growth response in regenerating liver and insulin-stimulated H-35 cells: comparison with serum-stimulated 3T3 cells and identification of 41 novel immediate-early genes.* Mol Cell Biol, 1991. **11**(1): p. 381-90.

11. Diamond, R.H., et al., *PRL-1, a unique nuclear protein tyrosine phosphatase, affects cell growth.* Mol Cell Biol, 1994. **14**(6): p. 3752-62.

12. Zeng, Q., W. Hong, and Y.H. Tan, *Mouse PRL-2 and PRL-3, two potentially prenylated protein tyrosine phosphatases homologous to PRL-1.* Biochem Biophys Res Commun, 1998. **244**(2): p. 421-7.

13. Sun, J.P., et al., *Phosphatase activity, trimerization, and the C-terminal polybasic region are all required for PRL1-mediated cell growth and migration.* J Biol Chem, 2007. **282**(39): p. 29043-51.

14. Zeng, Q., et al., *Prenylation-dependent association of protein-tyrosine phosphatases PRL-1, -2, and -3 with the plasma membrane and the early endosome.* J Biol Chem, 2000. **275**(28): p. 21444-52.

15. Fagerli, U.M., et al., *Overexpression and involvement in migration by the metastasis-associated phosphatase PRL-3 in human myeloma cells.* Blood, 2008. **111**(2): p. 806-15.

16. Basak, S., et al., *The metastasis-associated gene Prl-3 is a p53 target involved in cell-cycle regulation.* Mol Cell, 2008. **30**(3): p. 303-14.

17. Fiordalisi, J.J., P.J. Keller, and A.D. Cox, *PRL tyrosine phosphatases regulate rho family GTPases to promote invasion and motility.* Cancer Res, 2006. **66**(6): p. 3153-61.

18. Si, X., et al., *Interaction of farnesylated PRL-2, a protein-tyrosine phosphatase, with the beta-subunit of geranylgeranyltransferase II.* J Biol Chem, 2001. **276**(35): p. 32875-82.

19. Nishimura, A. and M.E. Linder, *Identification of a novel prenyl, palmitoyl CaaX modification of Cdc42 that regulates RhoGDI binding.* Mol Cell Biol, 2013.

20. Kozlov, G., et al., *Structural insights into molecular function of the metastasis-associated phosphatase PRL-3.* J Biol Chem, 2004. **279**(12): p. 11882-9.

21. Dumaual, C.M., et al., *Cellular localization of PRL-1 and PRL-2 gene expression in normal adult human tissues.* J Histochem Cytochem, 2006. **54**(12): p. 1401-12.

22. Rundle, C.H. and C. Kappen, *Developmental expression of the murine Prl-1 protein tyrosine phosphatase gene.* J Exp Zool, 1999. **283**(6): p. 612-7.

23. Kong, W., et al., *PRL-1 PTPase expression is developmentally regulated with tissue-specific patterns in epithelial tissues.* Am J Physiol Gastrointest Liver Physiol, 2000. **279**(3): p. G613-21.

24. Dong, Y., et al., *Phosphatase of regenerating liver 2 (PRL2) is essential for placenta development by downregulating PTEN (phosphatase and tensin homologue deleted on chromosome 10) and activating Akt.* J Biol Chem, 2012. **287**(38): p. 32172-9.

25. Matter, W.F., et al., *Role of PRL-3, a human muscle-specific tyrosine phosphatase, in angiotensin-II signaling.* Biochem Biophys Res Commun, 2001. **283**(5): p. 1061-8.

26. Guo, K., et al., *PRL-3 initiates tumor angiogenesis by recruiting endothelial cells in vitro and in vivo.* Cancer Res, 2006. **66**(19): p. 9625-35.

27. Molleví, D.G., et al., *PRL-3 is essentially overexpressed in primary colorectal tumours and associates with tumour aggressiveness.* Br J Cancer, 2008. **99**(10): p. 1718-25.

28. Wang, Y., et al., *Expression of the human phosphatases of regenerating liver (PRLs) in colonic adenocarcinoma and its correlation with lymph node metastasis.* Int J Colorectal Dis, 2007. **22**(10): p. 1179-84.

29. Laurent, C., et al., *High PTP4A3 phosphatase expression correlates with metastatic risk in uveal melanoma patients.* Cancer Res, 2011. **71**(3): p. 666-674.

30. Kong, L., et al., *The value and correlation between PRL-3 expression and matrix metalloproteinase activity and expression in human gliomas.* Neuropathology, 2007. **27**(6): p. 516-21.

31. Lu, J.W., et al., *Increased expression of PRL-1 protein correlates with shortened patient survival in human hepatocellular carcinoma.* Clin Transl Oncol, 2012. **14**(4): p. 287-93.

32. Hwang, J.J., et al., *Altered expression of phosphatase of regenerating liver gene family in non-small cell lung cancer.* Oncol Rep, 2012. **27**(2): p. 535-40.

33. Kato, H., et al., *High expression of PRL-3 promotes cancer cell motility and liver metastasis in human colorectal cancer: a predictive molecular marker of metachronous liver and lung metastases.* Clin Cancer Res, 2004. **10**(21): p. 7318-28.

34. Liu, Y.Q., et al., *Expression of phosphatase of regenerating liver 1 and 3 mRNA in esophageal squamous cell carcinoma.* Arch Pathol Lab Med, 2008. **132**(8): p. 1307-12.

35. Hardy, S., et al., *Overexpression of the protein tyrosine phosphatase PRL-2 correlates with breast tumor formation and progression.* Cancer Res, 2010. **70**(21): p. 8958-67.

36. Zhou, J., et al., *Over-expression of phosphatase of regenerating liver-3 correlates with tumor progression and poor prognosis in nasopharyngeal carcinoma.* Int J Cancer, 2009. **124**(8): p. 1879-86.

37. Stephens, B., et al., *Small interfering RNA-mediated knockdown of PRL phosphatases results in altered Akt phosphorylation and reduced clonogenicity of pancreatic cancer cells.* Mol Cancer Ther, 2008. **7**(1): p. 202-10.

38. Akiyama, S., D. Dhavan, and T. Yi, *PRL-2 increases Epo and IL-3 responses in hematopoietic cells.* Blood Cells Mol Dis, 2010. **44**(4): p. 209-14.

39. Ooki, A., et al., *Therapeutic potential of PRL-3 targeting and clinical significance of PRL-3 genomic amplification in gastric cancer.* BMC Cancer, 2011. **11**(122).

40. Li, Z.R., et al., *Association of tyrosine PRL-3 phosphatase protein expression with peritoneal metastasis of gastric carcinoma and prognosis.* Surgery today, 2007. **37**(8): p. 646-51.

41. Miskad, U.A., et al., *High PRL-3 expression in human gastric cancer is a marker of metastasis and grades of malignancies: an in situ hybridization study.* Virchows Arch, 2007. **450**(2): p. 303-10.

42. Mayinuer, A., et al., *Upregulation of Protein Tyrosine Phosphatase Type IVA Member 3 (PTP4A3/PRL-3) is Associated with Tumor Differentiation and a Poor Prognosis in Human Hepatocellular Carcinoma.* Ann Surg Oncol, 2013. **20**(1): p. 305-17.

43. Zhao, W.B., et al., *Evaluation of PRL-3 expression, and its correlation with angiogenesis and invasion in hepatocellular carcinoma.* Int J Mol Med, 2008. **22**(2): p. 187-92.

44. Wang, Q., et al., *Analysis of stromal-epithelial interactions in prostate cancer identifies PTPCAAX2 as a potential oncogene.* Cancer Lett, 2002. **175**(1): p. 63-9.

45. Zhou, J., et al., *PRL-3, a metastasis associated tyrosine phosphatase, is involved in FLT3-ITD signaling and implicated in anti-AML therapy.* PLoS One, 2011. **6**(5): p. e19798.

46. Zhou, J., et al., *The pro-metastasis tyrosine phosphatase, PRL-3 (PTP4A3), is a novel mediator of oncogenic function of BCR-ABL in human chronic myeloid leukemia.* Mol Cancer, 2012. **11**(1): p. 72.

47. Ustaalioglu, B.B., et al., *Clinical importance of phosphatase of regenerating liver-3 expression in breast cancer.* Clin Transl Oncol, 2012. **14**(12): p. 911-22.

48. Hao, R.T., et al., *Prognostic and metastatic value of phosphatase of regenerating liver-3 in invasive breast cancer.* J Cancer Res Clin Oncol, 2010. **136**(9): p. 1349-57.

49. Radke, I., et al., *Expression and prognostic impact of the protein tyrosine phosphatases PRL-1, PRL-2, and PRL-3 in breast cancer.* Br J Cancer, 2006. **95**(3): p. 347-54.

50. Wang, L., et al., *Overexpression of phosphatase of regenerating liver-3 in breast cancer: association with a poor clinical outcome.* Ann Oncol, 2006. **17**(10): p. 1517-22.

51. Ma, Y. and B. Li, *Expression of phosphatase of regenerating liver-3 in squamous cell carcinoma of the cervix.* Med Oncol, 2011. **28**(3): p. 775-80.

52. Reich, R., S. Hadar, and B. Davidson, *Expression and clinical role of protein of regenerating liver (PRL) phosphatases in ovarian carcinoma.* Int J Mol Sci, 2011. **12**(2): p. 1133-45.

53. Polato, F., et al., *PRL-3 phosphatase is implicated in ovarian cancer growth.* Clin Cancer Res, 2005. **11**(19): p. 6835-9.

54. Guervós, M.A., et al., *Deletions of N33, STK11 and TP53 are involved in the development of lymph node metastasis in larynx and pharynx carcinomas.* Cell Oncol, 2007. **29**(4): p. 327-34.

55. Nielsen, T.O., et al., *Molecular characterisation of soft tissue tumours: a gene expression study.* Lancet, 2002. **359**(9314): p. 1301-7.

56. Broyl, A., et al., *Gene expression profiling for molecular classification of multiple myeloma in newly diagnosed patients.* Blood, 2010. **116**(14): p. 2543-53.

57. Min, S.H., et al., *Downregulation of p53 by phosphatase of regenerating liver 3 is mediated by MDM2 and PIRH2.* Life Sci, 2010. **86**(1-2): p. 66-72.

58. Jiang, Y., et al., *Phosphatase PRL-3 is a direct regulatory target of TGFbeta in colon cancer metastasis.* Cancer Res, 2011. **71**(1): p. 234-44.

59. Ikushima, H. and K. Miyazono, *TGFβ signalling: a complex web in cancer progression.* Nat Rev Cancer, 2010. **10**(6): p. 415-24.

60. Zheng, P., et al., *Snail as a key regulator of PRL-3 gene in colorectal cancer.* Cancer Biol Ther, 2011. **12**(8): p. 742-9.

61. Liu, Y., et al., *PRL-3 promotes epithelial mesenchymal transition by regulating cadherin directly.* Cancer Biol Ther, 2009. **8**(14): p. 1352-9.

62. Wang, H., et al., *PCBP1 suppresses the translation of metastasis-associated PRL-3 phosphatase.* Cancer Cell, 2010. **18**(1): p. 52-62.

63. Huo, L.R. and N. Zhong, *Identification of transcripts and translatants targeted by overexpressed PCBP1.* Biochim Biophys Acta, 2008. **1784**(11): p. 1524-33.

64. Guzińska-Ustymowicz, K. and A. Pryczynicz, *PRL-3, an emerging marker of carcinogenesis, is strongly associated with poor prognosis.* Anticancer Agents Med Chem, 2011. **11**(1): p. 99-108.

65. Liang, F., et al., *PRL3 promotes cell invasion and proliferation by down-regulation of Csk leading to Src activation.* J Biol Chem, 2007. **282**(8): p. 5413-9.

66. Liang, F., et al., *Translational control of C-terminal Src kinase (Csk) expression by PRL3 phosphatase.* J Biol Chem, 2008. **283**(16): p. 10339-46.

67. Ming, J., et al., *PRL-3 facilitates angiogenesis and metastasis by increasing ERK phosphorylation and up-regulating the levels and activities of Rho-A/C in lung cancer.* Pathology, 2009. **41**(2): p. 118-26.

68. Jian, M., et al., *Downregulating PRL-3 inhibit migration and invasion of lung cancer cell via RhoA and mDia1.* Tumori, 2012. **98**(3): p. 370-6.

69. Peng, L., et al., *PRL-3 promotes the motility, invasion, and metastasis of LoVo colon cancer cells through PRL-3-integrin beta1-ERK1/2 and-MMP2 signaling.* Mol Cancer, 2009. **8**(110).

70. Lee, S.K., et al., *Phosphatase of regenerating liver-3 promotes migration and invasion by upregulating matrix metalloproteinases-7 in human colorectal cancer cells.* Int J Cancer, 2012. **131**(3): p. E190-203.

71. Wang, H., et al., *PRL-3 down-regulates PTEN expression and signals through PI3K to promote epithelial-mesenchymal transition.* Cancer Res, 2007. **67**(7): p. 2922-6.

72. Forte, E., et al., *Ezrin is a specific and direct target of protein tyrosine phosphatase PRL-3.* Biochim Biophys Acta, 2008. **1783**(2): p. 334-44.

73. Bretscher, A., et al., *ERM-Merlin and EBP50 protein families in plasma membrane organization and functionv.* Annu Rev Cell Dev Biol, 2000. **16**: p. 113-43.

74. Bruce, B., et al., *Expression of the cytoskeleton linker protein ezrin in human cancers.* Clin Exp Metastasis, 2007. **24**(2): p. 69-78.

75. Peng, L., et al., *Identification of integrin alpha1 as an interacting protein of protein tyrosine phosphatase PRL-3.* Biochem Biophys Res Commun, 2006. **342**(1): p. 179-83.

76. Krndija, D., et al., *The phosphatase of regenerating liver 3 (PRL-3) promotes cell migration through Arf-activity-dependent stimulation of integrin α5 recycling.* J Cell Sci, 2012. **125**(Pt 16): p. 3883-92.

77. Semba, S., E. Mizuuchi, and H. Yokozaki, *Requirement of phosphatase of regenerating liver-3 for the nucleolar localization of nucleolin during the progression of colorectal carcinoma.* Cancer Sci, 2010. **101**(10): p. 2254-61.

78. Zheng, P., et al., *Stathmin, a new target of PRL-3 identified by proteomic methods, plays a key role in progression and metastasis of colorectal cancer.* J Proteome Res, 2010. **9**(10): p. 4897-905.

79. McParland, V., et al., *The metastasis-promoting phosphatase PRL-3 shows activity toward phosphoinositides.* Biochemistry, 2011. **50**(35): p. 7579-90.

80. Pathak, M.K., et al., *Pentamidine is an inhibitor of PRL phosphatases with anticancer activity.* Mol Cancer Ther, 2002. **1**(14): p. 1255-64.

81. Daouti, S., et al., *A selective phosphatase of regenerating liver phosphatase inhibitor suppresses tumor cell anchorage-independent growth by a novel mechanism involving p130Cas cleavage.* Cancer Res, 2008. **68**(4): p. 1162-9.

82. Ahn, J.H., et al., *Synthesis and biological evaluation of rhodanine derivatives as PRL-3 inhibitors.* Bioorg Med Chem Lett, 2006. **16**(11): p. 2996-9.

83. Wang, L., et al., *An anticancer effect of curcumin mediated by down-regulating phosphatase of regenerating liver-3 expression on highly metastatic melanoma cells.* Mol Pharmacol, 2009. **76**(6): p. 1238-45.

84. Guo, K., et al., *Monoclonal antibodies target intracellular PRL phosphatases to inhibit cancer metastases in mice.* Cancer Biol Ther, 2008. **7**(5): p. 750-7.

85. Guo, K., et al., *Targeting intracellular oncoproteins with antibody therapy or vaccination.* Sci Transl Med, 2011. **3**(99): p. 99ra85.

86. Guo, K., et al., *Engineering the first chimeric antibody in targeting intracellular PRL-3 oncoprotein for cancer therapy in mice.* Oncotarget, 2012. **3**(2): p. 158-71.

87. Liu, P., N.A. Jenkins, and N.G. Copeland, *A highly efficient recombineering-based method for generating conditional knockout mutations.* Genome Res, 2003. **13**(3): p. 476-84.

88. Sauer, B. and N. Henderson, *Site-specific DNA recombination in mammalian cells by the Cre recombinase of bacteriophage P1.* Proc Natl Acad Sci U S A, 1988. **85**(14): p. 5166-70.

89. Nagy, A., et al., *Derivation of completely cell culture-derived mice from early-passage embryonic stem cells.* Proc Natl Acad Sci U S A, 1993. **90**(18): p. 8424-8.

90. Chandra, D., et al., *GABAA receptor alpha 4 subunits mediate extrasynaptic inhibition in thalamus and dentate gyrus and the action of gaboxadol.* Proc Natl Acad Sci U S A, 2006. **103**(41): p. 15230-5.

91. Ramírez-Solis, R., P. Liu, and A. Bradley, *Chromosome engineering in mice.* Nature, 1995. **378**(6558): p. 720-4.

92. Orban, P.C., D. Chui, and J.D. Marth, *Tissue- and site-specific DNA recombination in transgenic mice.* Proc Natl Acad Sci U S A, 1992. **89**(15): p. 6861-6865.

93. Wu, S., et al., *A protocol for constructing gene targeting vectors: generating knockout mice for the cadherin family and beyond.* Nat Protoc, 2008. **3**(6): p. 1056-76.

94. Rodríguez, C.I., et al., *High-efficiency deleter mice show that FLPe is an alternative to Cre-loxP.* Nat Genet, 2000. **25**(2): p. 139-40.

95. Lakso, M., et al., *Efficient in vivo manipulation of mouse genomic sequences at the zygote stage.* Proc Natl Acad Sci U S A, 1996. **93**(12): p. 5860-5.

96. Silva, A.J., et al., *Mutant mice and neuroscience: recommendations concerning genetic background. Banbury Conference on genetic background in mice.* Neuron, 1997. **19**(4): p. 755-9.

97. Reed, D.R., M.P. Lawler, and M.G. Tordoff, *Reduced body weight is a common effect of gene knockout in mice.* BMC Genet, 2008. **9**(4).

98. Kanneganti, M., M. Mino-Kenudson, and E. Mizoguchi, *Animal models of colitis-associated carcinogenesis.* J Biomed Biotechnol, 2011. **2011**.

99. Neufert, C., C. Becker, and M.F. Neurath, *An inducible mouse model of colon carcinogenesis for the analysis of sporadic and inflammation-driven tumor progression.* Nat Protoc, 2007. **2**(8): p. 1998-2004.

100. O'Toole, S.M., A.E. Pegg, and J.A. Swenberg, *Repair of O6-methylguanine and O4-methylthymidine in F344 rat liver following treatment with 1,2-dimethylhydrazine and O6-benzylguanine.* Cancer Res, 1993. **53**(17): p. 3895-8.

101. Kohno, H., et al., *Beta-Catenin mutations in a mouse model of inflammation-related colon carcinogenesis induced by 1,2-dimethylhydrazine and dextran sodium sulfate.* Cancer Sci, 2005. **96**(2): p. 69-76.

102. De Robertis, M., et al., *The AOM/DSS murine model for the study of colon carcinogenesis: From pathways to diagnosis and therapy studies.* J Carcinog, 2011. **10**(9).

103. Guda, K., et al., *Defective processing of the transforming growth factor-beta1 in azoxymethane-induced mouse colon tumors.* Mol Carcinog, 2003. **37**(1): p. 51-59.

104. Chen, H., et al., *Mitofusins Mfn1 and Mfn2 coordinately regulate mitochondrial fusion and are essential for embryonic development.* J Cell Biol, 2003. **160**(2): p. 189-200.

105. Eilers, M., et al., *Chimaeras of myc oncoprotein and steroid receptors cause hormone-dependent transformation of cells.* Nature, 1989. **340**(6228): p. 66-8.

106. Massagué, J., *TGFβ in Cancer.* Cell, 2008. **134**(2): p. 215-30.

107. Zhu, Y., et al., *Smad3 mutant mice develop metastatic colorectal cancer.* Cell, 1998. **94**(6): p. 703-14.

108. Takaku, K., et al., *Intestinal tumorigenesis in compound mutant mice of both Dpc4 (Smad4) and Apc genes.* Cell, 1998. **92**(5): p. 645-56.

109. Zimmerman, M.W., G.E. Homanics, and J.S. Lazo, *Targeted deletion of the metastasis-associated phophatase Ptp4a3 (PRL-3) suppresses murine colon cancer.* PLoS ONE, 2013. **8**(3): p. e58300.

110. Stephens, B.J., et al., *PRL phosphatases as potential molecular targets in cancer.* Mol Cancer Ther, 2005. **4**(11): p. 1653-61.

111. St Croix, B., et al., *Genes expressed in human tumor endothelium.* Science, 2000. **289**(5482): p. 1197-202.

112. Bardelli A, S.S., Sager JA, Romans KE, Xin B, Markowitz SD, Lengauer C, Velculescu VE, Kinzler KW, Vogelstein B., *PRL-3 expression in metastatic cancers.* Clin Cancer Res, 2003. **9**(15): p. 5607-15.

113. Parker, B.S., et al., *Alterations in vascular gene expression in invasive breast carcinoma.* Cancer Res, 2004. **64**(21): p. 7857-66.

114. He, H., et al., *Vascular endothelial growth factor signals endothelial cell production of nitric oxide and prostacyclin through flk-1/KDR activation of c-Src.* J Biol Chem, 1999. **274**(35): p. 25130-5.

115. Rousseau, S., et al., *p38 MAP kinase activation by vascular endothelial growth factor mediates actin reorganization and cell migration in human endothelial cells.* Oncogene, 1997. **15**(18): p. 2169-77.

116. Xu, J., et al., *VEGF promotes the transcription of the human PRL-3 gene in HUVEC through transcription factor MEF2C.* PLoS One, 2011. **6**(11): p. e27165.

117. Isenberg, J.S., et al., *Thrombospondin-1 inhibits endothelial cell responses to nitric oxide in a cGMP-dependent manner.* Proc Natl Acad Sci, 2005. **102**(37): p. 13141-6.

118. Tyurina, Y.Y., et al., *Oxidative lipidomics of γ-radiation-induced lung injury: mass spectrometric characterization of cardiolipin and phosphatidylserine peroxidation.* Radiat Res, 2011. **175**(5): p. 610-12.

119. Hainaud, P., et al., *The role of the vascular endothelial growth factor-Delta-like 4 ligand/Notch4-ephrin B2 cascade in tumor vessel remodeling and endothelial cell functions.* Cancer Res, 2006. **66**(17): p. 8501-10.

120. Zeng, Q., et al., *PRL-3 and PRL-1 promote cell migration, invasion, and metastasis.* Cancer Res, 2003. **63**(11): p. 2716-22.

121. Stempien-Otero, A., et al., *Mechanisms of hypoxia-induced endothelial cell death. Role of p53 in apoptosis.* J Biol Chem, 1999. **274**(12): p. 8039-45.

122. Choi, M.S., et al., *The essential role of FKBP38 in regulating phosphatase of regenerating liver 3 (PRL-3) protein stability.* Biochem Biophys Res Commun, 2011. **406**(2): p. 305-9.

123. Dormond, O., J.C. Madsen, and D.M. Briscoe, *The effects of mTOR-Akt interactions on anti-apoptotic signaling in vascular endothelial cells.* J Biol Chem, 2007. **282**(32): p. 23679-86.

124. Hurwitz, H., et al., *Bevacizumab plus irinotecan, fluorouracil, and leucovorin for metastatic colorectal cancer.* N Engl J Med, 2004. **350**(23): p. 2335-42.

125. Sandler, A., et al., *Paclitaxel-carboplatin alone or with bevacizumab for non-small-cell lung cancer.* N Engl J Med, 2006. **355**(24): p. 2542-50.

126. Escudier, B., et al., *Sorafenib in advanced clear-cell renal-cell carcinoma.* N Engl J Med, 2007. **356**(2): p. 125-34.

127. Casanovas, O., et al., *Drug resistance by evasion of antiangiogenic targeting of VEGF signaling in late-stage pancreatic islet tumors.* Cancer Cell, 2005. **8**(4): p. 299-309.

128. Madison, B.B., et al., *Cis elements of the villin gene control expression in restricted domains of the vertical (crypt) and horizontal (duodenum, cecum) axes of the intestine.* J Biol Chem, 2002. **277**(36): p. 33275-83.